The Effect of Antibiotic Resistance Genes (ARGs) on The Dynamics of Diverse Bacterial Populations

A thesis presented in partial fulfilment of the requirements for the degree of

Master of Science

in

Biological Sciences

at Massey University, Albany

New Zealand

Razvan Mihai Hancu

2025

Abstract

Antibiotic resistance genes (ARGs) represent a significant threat to global public health by compromising the effectiveness of antibiotics. Understanding how ARGs affect the dynamics of bacterial communities is essential for predicting how resistance may persist and spread, especially in environments without antibiotic selection pressure. This study examines how ARGs influence bacterial fitness across various genetic backgrounds and community structures, providing insights into the complex interactions driving antibiotic resistance.

In this study, six distinct bacterial strains—*Escherichia coli REL606* and five natural isolates—were first genetically tagged with unique chromosomal barcodes, enabling precise identification and tracking using high-throughput nanopore sequencing. Then, the barcoded sub-derivative strains were paired with plasmids carrying one of six ARGs (*aadA, bla*$_{TEM\text{-}116*}$*, bla*$_{CTX\text{-}M\text{-}15}$*, bla*$_{SHV\text{-}12}$*, cat, dfrA5*) or a control vector. This approach allowed for a detailed analysis of the fitness effects associated with different ARGs across multiple strains and competitive contexts.

Experimental results demonstrated clear fitness costs linked to the carriage of ARGs, although these costs varied significantly depending on the bacterial strain and the specific ARG involved. From the six ARGs tested, four (*aadA, bla*$_{CTX\text{-}M\text{-}15}$*, cat, dfrA5*) consistently imposed significant fitness burdens on their bacterial hosts. It is worth mentioning that the interactions between ARGs and host genetic backgrounds played an important role, underscoring the strain-specific nature of resistance.

Furthermore, the composition of bacterial communities had a strong influence on the fitness effects of ARGs. Experiments ranging from simple pairwise competitions to more complex multi-strain interactions highlighted the significant role of community context in determining the persistence of ARGs and competitive bacterial success.

Overall, this research provides valuable new insights into the intricate relationships between ARGs, bacterial genetic diversity, and community composition context, offering valuable insights for developing targeted strategies to manage and mitigate antibiotic resistance.

Acknowledgements

First and foremost, I want to thank my partner for being incredibly supportive and patient, especially in enduring my endless whining and complaining about the challenges I faced during my Master's thesis journey. Your pragmatic two-option solution gave me all the encouragement and reassurance I needed.

I am grateful to my parents, whose constant encouragement and belief in me kept my motivation alive, particularly during those tougher moments when the finish line seemed out of reach.

My sincere thanks go to my main supervisor, Tim Cooper, for his exceptional guidance, pastoral care, and insightful advice throughout this journey. Tim continually challenged me to think outside the box, helped me recognise the limitations of my project, and guided me in navigating complex situations. His invaluable assistance with the very complex R scripts and his thoughtful direction in shaping this thesis were critical to its completion.

I am equally grateful to my secondary supervisor, Evelyn Sattlegger, for stepping in and picking up the pieces when the College of Science unexpectedly shut its doors halfway through my work on this thesis.

Although navigating the uncertainties surrounding the College's closure was challenging, the support from supervisors and colleagues significantly eased the process. I would also like to express my sincere appreciation to my lab mates for their invaluable help, friendship, and the many experiences we shared. A special thanks to Huei-Yi Lai, whose help, expertise and advice were instrumental in constructing the barcoded derivatives used in this study. I would also like to acknowledge and thank Liza Lobko for her assistance with the initial testing of the barcoding method.

To Sean McFadyen, thank you for the great chats, the banter, and especially for generously allowing me to use your supercomputer to basecall the extensive sequencing data generated during this project. Matthew Adlam, your advice, particularly on R scripting, along with your good humour and friendly chats, made the lab experience genuinely enjoyable.

Special thanks to Olin Silander and Nick McGrath for their invaluable support and expertise with nanopore sequencing techniques. Lastly, my gratitude extends to all the fellow students and staff whose support, kind gestures, words of encouragement, and smiles made this journey significantly more manageable and enjoyable.

Abbreviations

Amp – Ampicillin

AMR – Antimicrobial Resistance

ANOVA – Analysis of Variance

ARG(s) – Antibiotic Resistance Gene(s)

ARMs – Antibiotic Resistance Mutations

bp – Base pairs

BSA – Bovine Serum Albumin

CFU – Colony Forming Unit

CI – Confidence Interval

DNA – Deoxyribonucleic Acid

dsDNA – Double-stranded DNA

Flp – Flippase recombinase (site-specific recombinase)

GFP – Green Fluorescent Protein

Gm – Gentamicin

Gm^R – Gentamicin resistance

gDNA – Genomic DNA

HGT – Horizontal Gene Transfer

Km – Kanamycin

Km^R – Kanamycin resistance

LB – Lysogeny Broth

MGE(s) – Mobile Genetic Element(s)

MRG(s) – Metal Resistance Gene(s)

NGS – Next Generation Sequencing

Nx – Nalidixic acid

ONT – Oxford Nanopore Technologies

PCR – Polymerase Chain Reaction

PBP – Penicillin Binding Protein

PRP(s) – Pheromone Responsive Plasmid(s)

QC – Quality Control

RBK – Rapid Barcoding Kit

rDNA – Ribosomal DNA

rRNA – Ribosomal RNA

Rpm – Revolutions per minute

SDS – Sodium Dodecyl Sulfate

Tm – Melting Temperature

VGT – Vertical Gene Transfer

Table of Contents

Abstract ***2***

Acknowledgements ***3***

Abbreviations ***4***

List of figures ***9***

List of tables ***10***

Chapter 1: Introduction ***11***

1.1 Background and significance **11**

1.2 Genetic origins and dissemination of antibiotic resistance **12**

1.2.1 Genetic pathways to antibiotic resistance 12

1.2.2 HGT as a vehicle for the dissemination of ARGs 13

1.2.3 Plasmids are the most common vector for ARGs 14

1.3 Fitness costs of ARGs **17**

1.4 The influence of the host strain on the success of ARGs **18**

1.5 Community dynamics **20**

1.5.1 Malthusian (exponential) growth theory. 22

1.6 Barcodes – high resolution tool to track subtle changes in the community. **23**

1.7 Research objectives **24**

Chapter 2: Materials and methods ***26***

2.1 Strains and ARGs **26**

2.1.1 Strains 26

2.1.2 ARGs 26

2.2 Barcode constructs **29**

2.2.1 Construction of the Tn7 integration plasmid 31

2.2.2 Chromosomal integration of the barcode 34

2.2.3 Selection marker excision from the chromosomal barcode cassette 37

2.2.5 Construction of barcoded ARG sub-derivatives 38

2.3 Plasmid loss test **38**

2.4 Plasmid transfer test **39**

2.5 Competition setup 40

2.6 Competition types 40

2.6.1 Competition Between a Single Strain Carrying a Single ARG (one ARG – one strain) 41

2.6.2 Competition Among All Six ARGs in a Single Strain (all ARGs – one strain) 41

2.6.3 Competition Among Different Strains Carrying The Same ARG (one ARG – all strains) 41

2.6.4 Competition Among All ARGs And All Strains (all ARGs – all strains) 42

2.6.5 Competition Among All Strains Carrying Only The Vectors (all strains – vector) 42

2.7 PCR amplification 42

2.7.1 PCR clean up 44

2.8 Oxford Nanopore sequencing 45

2.8.1 Library preparation using Rapid Barcoding Kit 96 V14 45

2.8.2 Sequencing on PromethION 2 Solo 46

2.9 Basecalling and data analysis 46

2.9.1 Basecalling 46

2.9.2 Demultiplexing 47

2.9.3 Data analysis 47

Chapter 3: Results 50

3.1 No significant plasmid loss or transfer was detected 50

3.2 Processing barcode sequencing data and evaluating barcode fidelity 51

3.3 Comparison of the fluorescent marker and barcode frequency methods for estimating ARG fitness effects 53

3.4 Fitness effects of ARGs 55

3.4.1 ARGs impose costs on their hosts in environments without selection pressure from antibiotics. 55

3.4.2 Fitness effects are strain dependent. 58

3.4.3 Fitness variation is driven by ARG-strain interactions in pairwise competitions. 58

3.5 Community composition affects the cost of resistance. 62

3.5.1 The fitness effects of ARGs depend on the specific competition environment. 62

3.5.2 The fitness effects of ARGs depend on the host strain and vary across different competition types. 65

3.5.3 ARG fitness effects are shaped by strain identity and competition type. 69

Chapter 4: Discussion 70

4.1 Strain-specific fitness effects 70

4.2 Community context determines the success of ARGs and strains. 71

4.3 Strains, ARGs and the community context.....72

4.4 Extension beyond ARGs: Costs of accessory gene expression in the mobile plasmidome.....74

4.5 Future research and conclusion.....77

Supplementary data 79

REFERENCES.....88

List of figures

Figure 1. **Overview of barcoding steps to construct the barcode libraries**. 30

Figure 2. **Primer binding sites within the barcoded integration plasmid**. 33

Figure 3 A. Map of the Tn7 helper plasmid & B. Map of the Tn7 barcode integration plasmid 35

Figure 4. **Comparison of fitness estimates for ARGs using fluorescent marker and barcode frequency methods** 54

Figure 5. **Mean fitness effects of ARGs compared to the vector control**. 56

Figure 6. **Mean fitness effects of ARGs in each strain**. 60

Figure 7. **Fitness effect of each ARG in each strain**. 61

Figure 8. **Fitness effect of each ARG across all strains in different competition types**. 63

Figure 9. **ARGs effect on strains across different competition types**. 66

Figure 10. **Mean fitness effects of ARGs relative to vector controls across different competition types and host strains** 69

List of tables

Table 1. **ARGs used in this study**.....28
Table 2. **PCR primers used to amplify the vector plasmid**.. 32
Table 3. **Primers designed to amplify the 500 bp barcode region of the chromosome**.....44
Table 4. **Summary of plasmid loss percentages and statistical significance across strains**. 51
Table 5. **Mean fitness effects of ARGs compared to vector**.....57
Table 6. **Summary of fitness effects of ARGs in different competition environments**. 64
Table 7. **Summary of host strain fitness effects in different competition environments**....67
Supplementary Table 1. **Summary statistics of colony counts in plasmid transfer assay**. ...79
Supplementary Table 2. **Dunnett's Test Results for the Fitness Effects of ARGs Relative to the Vector Control**. 81
Supplementary Table 3. **Wilcoxon test comparison between competition types for each ARG (BH correction).**.....83
Supplementary Table 4. **Wilcoxon test comparison between competition types for each strain (BH correction).** 85

Chapter 1: Introduction

1.1 Background and significance

Antibiotic resistance genes (ARGs) are present in almost all environments (Wang et al., 2019; Zhuang et al., 2021). The use of antibiotics in health care and agriculture has contributed to the selection and dissemination of these genes in bacterial communities. ARGs represent a significant threat to public health as they cause antibiotics to be ineffective against bacterial infections (Bengtsson-Palme et al., 2017; Duan et al., 2020; Parker et al., 2024). However, knowledge of the role of ARGs in promoting antimicrobial resistance is not enough to understand their success since the use of antibiotics is not the only factor that affects the maintenance and evolution of ARGs; it is also necessary to study the costs ARGs have in the absence of antibiotics. Such costs may cause reduced growth rates or other negative effects on fitness when bacteria carry these genes in an antibiotic-free environment (Hernando-Amado et al., 2017). Examining how ARGs influence bacterial fitness and persistence, particularly within microbial communities that are not exposed to antibiotics, is essential to fully understand how antibiotic resistance can be maintained in diverse bacterial communities. Previous research on antibiotic resistance mutations has shown that fitness costs can vary substantially between host strains; a particular mutation might impose significant burdens on one bacterial strain but negligible effects on another (Vogwill et al., 2016). It is likely that resistance genes carried on plasmids exhibit similar strain-dependent fitness effects, although this remains less well studied. This raises a key question: do the fitness costs of ARGs depend solely on the carrying host strain, or are they also influenced by interactions within the broader bacterial community? Understanding how host–gene interactions are shaped by community context is crucial for predicting the persistence and spread of antibiotic resistance genes.

1.2 Genetic origins and dissemination of antibiotic resistance

1.2.1 Genetic pathways to antibiotic resistance

Bacteria can acquire antibiotic resistance through two primary genetic pathways: antibiotic resistance mutations (ARMs) and antibiotic resistance genes (ARGs). These two pathways are very different in their genetic origins and evolutionary implications.

Antibiotic resistance mutations (ARMs) arise spontaneously within the bacterial genome from errors during DNA replication or due to exposure to mutagenic agents (Gifford et al., 2023). ARMs can be found within a bacterial population as pre-existing genetic diversity before antibiotic exposure or they can develop spontaneously during antibiotic treatment. ARMs provide bacteria with adaptive advantages in the presence of antibiotics by altering drug targets, enhancing efflux mechanisms, or reducing drug uptake (Blair et al., 2015; Hughes & Andersson, 2015; Melnyk et al., 2015). ARMs can have evolutionary implications because they can rapidly occur within a population under selective pressure from exposure to antibiotic. However, ARMs often impose a fitness cost when antibiotics are not present. These costs can limit their persistence in natural environments, although costs can often be compensated (Andersson & Hughes, 2010; Melnyk et al., 2015).

Antibiotic resistance genes (ARGs) are acquired through horizontal gene transfer (HGT), a process that allows bacteria to obtain genetic material from other organisms or the environment through plasmids, transposons, and integrons (Partridge et al., 2018). ARGs provide resistance through mechanisms that degrade or modify antibiotics, alter antibiotic targets, or eliminate antibiotics from the cell. For example, β-lactamases hydrolyse the β-lactam ring of penicillins and cephalosporins (Bush, 2012; de Souza et al., 2024), while aminoglycoside-modifying enzymes alter aminoglycosides to prevent binding to ribosomal targets (Ramirez & Tolmasky, 2010). ARGs can also encode proteins that alter targets, such as penicillin-binding proteins (PBPs) that reduce the binding affinity of β-lactam antibiotics (Sun et al., 2014) or modify ribosomal RNA to prevent binding of macrolides and tetracyclines (Leclercq, 2002). Efflux pumps encoded by ARGs expel a wide range of antibiotics, including

tetracyclines and fluoroquinolones, therefore reducing their intracellular concentrations (Li & Nikaido, 2009; Poole, 2007). ARGs are believed to originate from environmental microbiomes where antibiotics are naturally produced (Martínez et al., 2015). The dissemination of ARGs through HGT has significant evolutionary implications since it allows resistance traits to spread rapidly across all bacterial species, therefore contributing to the emergence of multidrug-resistant strains.

Although not explored in detail here, vertical gene transfer (VGT) is another important mechanism. Vertical transfer of ARGs refers to the passing of resistance determinants from a parent bacterium to its offspring during replication (cell division), so that the progeny inherit those ARGs (Galgano et al., 2025). Intrinsic resistance genes are innate, chromosomally encoded traits of a bacterial species (universally present in that species) that confer natural antibiotic resistance without prior exposure and are passed on largely through VGT, whereas acquired resistance genes are those gained later through HGT or mutations, introducing new resistance traits not originally found in that species (Galgano et al., 2025).

1.2.2 HGT as a vehicle for the dissemination of ARGs

HGT is a mechanism bacteria use to acquire genetic material from other organisms rather than relying on inheritance from their parents. It allows the rapid dissemination of ARGs in bacterial populations and environments (von Wintersdorff et al., 2016). The main mechanisms of HGT are transformation, transduction, and conjugation (Brüssow et al., 2004; Chen & Dubnau, 2004; Smillie et al., 2010). These mechanisms often facilitate the mobilisation and accumulation of ARGs; importantly, their activity can be significantly enhanced under the selective pressure from the presence of antibiotics in the environment, which accelerates the spread of ARGs through HGT. For example, the presence of antibiotics can induce the SOS response in bacteria, which in turn increases the rates of mutation and HGT mechanisms (Beaber et al., 2004).

Studies have found a direct correlation between the contamination of the environment with antibiotics and the prevalence of ARGs. For example, areas with high levels of antibiotic contamination, such as wastewater treatment plants and agricultural fields treated with

manure, exhibit a marked increase in the diversity and abundance of ARGs (Deng et al., 2020; Xiong et al., 2015). Manure-amended soils, which are rich in both antibiotics and resistant bacteria, serve as hotspots for HGT and facilitate the spread of ARGs to native microbial communities (Hu et al., 2017). Another example is the introduction of tetracyclines into aquatic sediments, which greatly increased the presence of the *tetA* resistance gene. These genes were maintained long after the antibiotic treatment, which highlights the long-lasting impact on the spread of ARGs (Deng et al., 2020). Additionally, plasmids such as the IncP-1 family are able to carry multiple ARGs that can be transferred between diverse bacterial hosts, significantly contributing to the spread of resistance genes and multi-drug resistance in various environments (Heuer et al., 2012).

HGT is the primary vehicle for the dissemination of ARGs across diverse ecological environments, and it can be intensified by the selective pressures imposed by antibiotics (Ellabaan et al., 2021; Hu et al., 2017).

1.2.3 Plasmids are the most common vector for ARGs

Plasmids are extrachromosomal DNA elements capable of self-replication within bacterial cells and are recognised as the primary vectors for the dissemination of ARGs (Carattoli, 2013; Partridge et al., 2018). Their ability to transfer between bacteria through HGT, highlights their important role in the spread of antibiotic resistance (Partridge et al., 2018; Smillie et al., 2010).

Plasmids are often classified by their ability to transfer themselves or by their reliance on external factors for transfer. Self-transmissible or conjugative plasmids carry genes that encode the machinery necessary for their own transfer, including the origin of transfer (oriT) and transfer genes (*tra* genes). These plasmids can transfer themselves to other bacteria, promoting the spread of ARGs across diverse bacterial populations and environments (Smillie et al., 2010). In contrast, mobilisable plasmids lack the necessary transfer genes and rely on the presence of helper plasmids (self-transmissible plasmids) within the same cell for their transfer (Smillie et al., 2010). This interdependence can facilitate the co-transfer of multiple resistance determinants and complicate efforts to control antibiotic resistance (Carattoli, 2013; Partridge et al., 2018). Non-transmissible plasmids have no ability to transfer through

conjugation or be mobilised, so they are either passed on vertically or through transformation or transduction (Smillie et al., 2010).

The copy number of plasmids is defined as the average number of plasmid molecules present per bacterial cell, which significantly influences their impact on bacterial fitness and the stability of ARGs. Plasmids with low-copy-number (typically one to a few copies per cell) tend to impose a lower metabolic burden on the host cell, which can be advantageous for the maintenance of these plasmids over long periods(Ramiro-Martínez et al., 2025). Low-copy-number plasmids may have sophisticated partitioning systems to ensure they are inherited during cell division, therefore maintaining the presence of ARGs within bacterial populations (Nordstrom & Austin, 1989).

By contrast, plasmids with high-copy-number (tens to hundreds of copies per cell) can impose significant fitness costs on the host due to the metabolic burden of replicating and maintaining multiple plasmid copies. These costs can result in selection pressure for the loss of high-copy-number plasmids in the absence of antibiotic selective pressure (Millan & MacLean, 2017). Despite these fitness costs, high-copy-number plasmids can rapidly spread ARGs within bacterial populations under strong selective pressures, such as high antibiotic concentrations (Hernandez-Beltran et al., 2024).
The fitness effects of plasmid carriage are varied and depend on the environmental and genetic context. While plasmid-encoded ARGs can provide a selective advantage in the presence of antibiotics, the metabolic burden and potential disruption of host cellular processes can impose a fitness cost in antibiotic-free environments (Millan & MacLean, 2017). The spread and maintenance of antibiotic resistance do not depend only on the cost and benefits of plasmid carriage but also on the complex interplay between plasmids, bacterial hosts, and environmental factors (Bengtsson-Palme et al., 2017; Carattoli, 2013).

Plasmid genes can impose additional costs on their hosts and this can be an important factor in determining plasmid success. These costs can derive from disruptions to important cellular processes, interference with nutrient uptake, activation of stress responses and competition for the resources available for replication. For example, some plasmids can carry genes that produce toxic proteins, which can inhibit growth if the corresponding antitoxin genes are not

expressed at the same time (Gerdes et al., 1986; Van Melderen & Saavedra De Bast, 2009). Another source of burden comes from plasmid replication and partitioning functions. Large plasmids often carry their own origin of replication and partitioning (segregation) systems to ensure each daughter cell inherits the plasmid. These systems, however, co-opt the host's DNA polymerases, replication factors, and cytoskeletal elements for plasmid propagation. The result is a direct competition with the host chromosome for replication time and resources, which can slow down cell division and lower overall efficiency (Millan & MacLean, 2017). Plasmids can also carry metal resistance genes (MRGs) that help bacteria survive toxic metal exposure, but these genes can impose significant fitness costs on the host in metal-free conditions. Like antibiotic resistance, metal resistance mechanisms require the cell to express additional proteins (e.g. efflux pumps, metal-binding proteins, or detoxifying enzymes) that antagonise normal cellular processes when the metal stress is absent (Rouch et al., 1995; Silver, 1992). This burden can manifest as metabolic drain, membrane stress, and resource competition, ultimately slowing growth or reducing competitive fitness (Hall et al., 2015). These antagonistic interactions increase the overall metabolic cost imposed on host bacteria and shape the evolutionary trajectory of plasmids. As a result, the carriage of particularly costly genes becomes a critical factor determining whether plasmids persist and spread within bacterial populations.

1.3 Fitness costs of ARGs

The evolutionary success of ARGs is influenced by the biological costs these genes impose on bacterial hosts in antibiotic-free environments, and it is not just a result of antibiotic pressure (Humphrey et al., 2012; Vogwill & MacLean, 2015). To understand the dynamics of ARG spread and persistence, it is important to understand the evolutionary trade-offs responsible for their success. Although studies highlight the existence of these costs (Hernando-Amado et al., 2017; Rajer et al., 2022), there is no detailed analysis of their overall impact on different bacterial populations, leaving a gap in our ability to predict ARGs behaviour under different antibiotic pressures. At the molecular level, the costs associated with antibiotic resistance often stem from the metabolic burden and fitness costs linked to the maintenance and expression of resistance genes and their associated mobile genetic elements (MGEs) (Millan & MacLean, 2017). While these costs can vary and can sometimes be compensated (Carroll & Wong, 2018), recent research has shifted focus towards understanding how ARGs and their interaction with host cellular processes dictate their fitness impact (Rajer et al., 2022). It is known that bacteria often pay a metabolic price for carrying ARGs in the absence of antibiotic pressure (Andersson & Hughes, 2010). For example, in one study, only two resistance genes ($bla_{CTX\text{-}M\text{-}15}$ and *tetAR*) on a multi-resistant plasmid were found to impose fitness costs. All the other resistance genes on the same plasmid had no measurable fitness effects, even when overexpressed (Rajer et al., 2022).

Several studies have demonstrated that ARGs can influence host physiology through multiple molecular mechanisms that extend beyond simple metabolic costs. For example, the acquisition or expression of certain ARGs in *E. coli* can interfere with DNA replication and transcription, which can cause the accumulation of RNA–DNA hybrids (R-loops) and DNA breaks, and subsequently trigger stress responses such as the SOS repair pathway (Balbontín et al., 2021). Similarly, the uptake of multidrug-resistance plasmids can cause strain-specific changes in gene expression, including activation of stress regulons, although without significant effects on growth (Dunn et al., 2021). Additionally, ARG-encoded proteins can impose stress when misfolded or unstable resistance proteins may accumulate and induce chaperone responses. In mycobacteria, the DnaK chaperone system buffers the fitness costs associated with rifampicin-resistance mutations by refolding or stabilising affected proteins

(Fay et al., 2021). ARGs can also induce cell-envelope stress when the overexpression of foreign efflux pumps disrupts membrane integrity due to excessive proton accumulation, requiring metabolic adjustments—such as activating anaerobic respiration pathways—to restore balance (Pacheco et al., 2017). Additionally, Liang et al. (2023) demonstrate how plasmid-borne lipid A-modifying enzymes like MCR-1 can alter membrane structure, simultaneously conferring antibiotic resistance, causing membrane stress and a measurable fitness cost (Liang et al., 2023). Genetic conflicts between ARGs and host regulatory systems have also been documented. For example, plasmid-encoded genes may trigger latent toxin–antitoxin systems or disrupt the balance of global regulators, causing fitness reductions that persist until compensatory mutations arise (Hall et al., 2021). Taken together, these findings highlight that fitness burdens associated with ARGs are complex and multifaceted, and can derive from transcriptional interference, protein misfolding stress, membrane disruption, metabolic adjustments, and alterations in host gene regulation. The detailed understanding of the costs associated with ARGs, particularly in competitive dynamics and independent of the plasmid context, is still not well studied.

1.4 The influence of the host strain on the success of ARGs

It is important to understand how the success of ARGs depends on the host strain in order to determine the impact ARGs have on fitness. The metabolic and physiological changes induced by ARGs can have varied effects on bacterial fitness and in turn influence the genomic landscape (Sánchez & Martínez, 2012). For example, these metabolic and physiological changes can reshape the genomic landscape by changing which bacterial genotypes thrive under selective pressures. ARG-related metabolic stress and fitness costs select for compensatory mutations that restore metabolic efficiency or otherwise reduce cellular burdens, enabling these genotypes to become dominant within populations (Durão et al., 2018). Additionally, bacteria carrying ARGs may adjust overall gene expression, downregulating costly metabolic pathways or virulence factors to offset energetic demands, in turn promoting the survival of strains that efficiently manage these trade-offs (Händel et al., 2014). In some scenarios, ARG-induced physiological adjustments can even confer unexpected fitness advantages; for instance, mutations associated with fluoroquinolone

resistance have been shown to enhance bacterial growth rates in *E. coli* and other Enterobacteriaceae, promoting the persistence and spread of these resistant genotypes within bacterial communities (Machuca et al., 2014).

However, the host can also determine the success of an ARG. The fitness impact of resistance genes varies across different host strains, which in turn influences the success of these genes (De Gelder et al., 2007; Humphrey et al., 2012). Research by Lai and Cooper underscores the complexity of antibiotic resistance dynamics and highlights that the fitness costs of ARGs are not fixed and vary significantly among different bacterial host strains and environments (Lai & Cooper, 2024). This variability can have a direct effect on the composition and persistence of both ARGs and strains within the community. Researchers have not examined the effect of the genetic background in detail, yet it could be a key factor in the success of ARGs.

1.5 Community dynamics

Interactions between species, and even strains of the same species, within bacterial communities are complicated and dynamic, and can have a significant effect on cell fitness. Differences in cell fitness will affect the composition of a community and may affect the evolution of antibiotic resistance (Alonso-del Valle et al., 2021). Interaction effects are non-linear, and the joint effects of a community are not always predicted by the sum of individual effects (Baichman-Kass et al., 2023; Geesink et al., 2024). Interactions that shape a community can range from cooperation (Colizzi & Hogeweg, 2016), where the exchange of genetic material or gene products aids members of the community, to competition (Hibbing et al., 2010), where bacteria eliminate members of the community to gain space and resources.

A classic example of interspecies cooperation is when bacteria acquire genetic material, including resistance genes, from neighbouring species in the community via HGT. *Enterococcus faecalis* is an endemic coloniser of the human gut and can have a significant role in the spread of antibiotic resistance by its capability of harbouring and transferring pheromone-responsive plasmids (PRPs). These plasmids can transfer ARGs or other virulence factors within or even between species (García-Solache & Rice, 2019). Therefore, such interspecies interactions driven by HGT can significantly amplify the spread of antibiotic resistance, posing considerable challenges to controlling resistance in bacterial communities.

Another type of interaction is syntrophy, a form of metabolic cooperation in which organisms cooperate to support each other's survival through metabolic byproducts that help them survive in certain environments (Morris et al., 2013). Syntrophy is essentially an obligate mutualism, meaning each partner requires the other’s contributions for growth. For example, two bacterial strains can engage in reciprocal cross-feeding of nutrients: each strain might be unable to synthesise a particular essential amino acid on its own, but it can obtain that amino acid from its partner while in turn providing a different amino acid that the partner needs (Mee et al., 2014). Through this bidirectional exchange, both organisms thrive together under conditions where neither would survive alone.

Cooperation among bacteria typically becomes more prevalent in environments where individual survival or growth is particularly challenging or energetically expensive. Under such stressful conditions—where resources are limited, competition is intense, or external pressures (e.g., high antibiotic concentrations) are substantial—bacteria often benefit by working collectively and sharing the costs of survival (Colizzi & Hogeweg, 2016). Similarly, when environmental stress or the energetic demands are low, bacterial populations often favour selfish behaviours, as individual cells can survive and grow efficiently without relying on cooperation (Colizzi & Hogeweg, 2016). For example, selfish resistance mechanisms like efflux pumps and target site modifications confer benefits only to the individual bacterial cell (Blair et al., 2015). Instead, cooperative resistance mechanisms like the secretion of β-lactamase enzymes provide communal benefits through the degradation of antibiotics from the environment (Blair et al., 2015).

In contrast, competition is a major force affecting the community structure. Competition can be direct, where one species will release toxins to kill the competing species, or indirect, where all compete for the same resources. An example of direct competition can be observed in the case of *Staphylococcus aureus* which uses its Type VII secretion system to produce a nuclease toxin EsaD to degrade the DNA of competing bacterial cells (Cao et al., 2016). The release of these toxins does not only change the structure of the microbial community but can also create selection pressure on the other bacteria driving the potential evolution of resistance mechanisms to survive the toxic attacks. When multiple bacterial species compete for limited resources, the selective pressure will favour strains that can utilise the resources more efficiently or adapt to poor nutrient availability. Butaitė et al. (2017) demonstrate in their study that *Pseudomonas* cheaters could outcompete others by depriving them of iron through the production of siderophores. In *Pseudomonas* communities, “cheaters” are mutants that avoid the metabolic cost of producing cooperative factors yet exploit those produced by others—examples include lasR mutants of *P. aeruginosa* that stop making quorum-sensing–controlled products and instead benefit from the public goods made by their wild-type partners (Sandoz et al., 2007) or pyoverdine-non-producing strains that scavenge iron by using siderophores secreted by neighbouring cells (Butaitė et al., 2017).

Lastly, quorum sensing is a communication mechanism bacteria use to respond to population density and involves the release and detection of chemical signalling molecules called autoinducers. For example, *Pseudomonas aeruginosa* use this mechanism to regulate the production of biofilms, which makes it more resistant to antibiotics by creating a physical barrier to slow the penetration of antimicrobial agents (Miranda et al., 2022).

1.5.1 Malthusian (exponential) growth theory.

In population biology, Malthusian growth refers to exponential population increase at a constant per-capita rate under conditions where resources are not yet limiting. This per-capita rate, often expressed as the Malthusian parameter, provides a natural logarithmic measure of growth over time (Concepción-Acevedo et al., 2015). Lenski and colleagues used an equivalent formulation in their long-term *E. coli* evolution experiment, where fitness was estimated from the change in relative frequencies of competing strains during a standard one-day competition assay (Lenski et al., 1991). Because the ratio of final to initial cell densities corresponds to the number of population doublings, comparing two strains' doublings over the same interval is mathematically equivalent to comparing their Malthusian parameters (Melnyk et al., 2015). This approach, rooted in classical Malthusian theory, has since become a widely used and rigorous method for quantifying microbial fitness in evolutionary and antibiotic-resistance studies.

1.6 Barcodes – high resolution tool to track subtle changes in the community.

To better understand the complex population dynamics occurring within defined communities we need to use new methods that enable accurate tracking of these dynamics and offer a high-resolution picture of the diverse and complex bacterial communities. For example, fluorescence-based cell sorting (e.g., GFP-tagging), qPCR, and various other molecular techniques (e.g., metagenomics) have been traditionally used to track bacterial population dynamics, but each has critical shortcomings. Fluorescence labelling (e.g., GFP-tagging) methods are constrained by a limited number of distinguishable markers and clonal interference, which severely restricts resolution for tracking more than a few lineages simultaneously (Hegreness et al., 2006; Kim, 2023; Kvitek & Sherlock, 2013). qPCR has limited multiplexing capability, which makes it less suited for high-throughput studies, and it is prone to bias due to primer efficiencies (Bustin & Nolan, 2017). Shotgun metagenomics usually provides community-level insights and struggles to differentiate closely related strains due to short-read assembly limitations and can miss strains with low relative abundance (Hillmann et al., 2018; Quince et al., 2017).

Chromosomal barcoding, a relatively new tool, allows for the integration of unique DNA sequences directly into the chromosomes of bacterial cells (Jasinska et al., 2020). These DNA sequences are known as barcodes and are introduced in neutral positions on the chromosome to uniquely label and track individual lineages within microbial populations (Levy et al., 2015). The main advantage of using chromosomal barcoding in tracking community and population dynamics is the ability to observe complex interactions within microbial communities at high-resolution (Nguyen Ba et al., 2019). The integration of next-generation sequencing (NGS) technologies with chromosomal barcoding has enabled a new way to efficiently sequence and quantify barcode frequencies within complex populations (Blundell & Levy, 2014; Theodosiou et al., 2023).

Chromosomal barcoding paired with the latest advancements in NGS promises a robust and precise method for tracking bacterial population dynamics and can be used to track how different antibiotic resistant strains compete within a community.

1.7 Research objectives

Although significant progress has been made in understanding the mechanisms behind antibiotic resistance and the factors that contribute to the spread of ARGs, there is still a gap in our understanding of how the composition of a bacterial community affects the persistence of ARGs in a focal host strain in an environment without antibiotics. I operationalise this question by testing if the fitness effect of an ARG on a focal host strain measured in a pairwise competition is changed in complex multi-strain competitions.

It has previously been established that interaction effects within bacterial communities can significantly influence fitness outcomes (Lai & Cooper, 2024; Nair & Andersson, 2023). Small changes in the frequency of strains carrying ARGs could potentially be amplified or mitigated due to these interaction effects, therefore influencing community structure and ARG maintenance. It is important to understand this sensitivity to these subtle frequency shifts to be able to predict how ARGs are maintained or lost in natural environments where bacterial populations are highly dynamic.

To investigate these interactions between a focal ARG carrying strain and the broader community we need sensitive tools that can capture the dynamics of bacterial populations in simple competition environments as well as more complex multi-strain competitions. Chromosomal barcoding represents a high-resolution tool that when paired with the latest available NGS technology can enable the precise tracking of individual bacterial cells within complex populations. By integrating unique DNA sequences into neutral regions of the bacterial chromosomes, I will be able to observe small changes in the frequency of these strains in all types of competitions, including multi-competitor communities. In these communities, some of the interactions described in section 1.5 can play an important role in the competition dynamics and, therefore, in the success of ARGs. For example, cross-feeding interactions may enable certain strains to thrive in the community by using metabolic byproducts from others, while allelopathic interactions may inhibit competitors. The high-resolution data observed in different complex community compositions paired with fitness of individual genotypes in simple pairwise competitions allowed me to test for the influence of broader ecological interactions.

My research aims to understand ARGs persistence in complex communities by investigating the effect of the host genetic background, evaluating the predictive ability of pairwise competitions in complex communities and exploring the sensitivity of community dynamics to small changes in the frequency of ARG-carrying strains.

Chapter 2: Materials and methods

2.1 Strains and ARGs

2.1.1 Strains

In this study, I focused on one laboratory strain of *Escherichia coli*, REL606, alongside five natural isolates: B156, H504, B354, H588, and M863. The natural isolates were chosen based on their ecological diversity: B156 is an *Escherichia albertii* strain isolated from magpie faeces (Oaks et al., 2010), M863 is a cryptic *Escherichia* clade I strain from a non-human source, while H504, H588, and B354 are commensal *E. coli* strains isolated from human hosts (Luo et al., 2011; Walk et al., 2009; Wang et al., 2016). The strains were selected based on their availability in our lab, available genome sequence, and ability to create fitness-neutral barcoded derivatives using the method outlined in Chapter 2.2. Although the genome sequences of some strains are available they have not been explored in this study but they could be useful in future research. Strain B156, one of the avian isolates studied by Oaks et al. was identified as *E. albertii*, a species that shares many phenotypic and genetic features with *E. coli* yet is distinct at the species level (Gomes et al., 2020). Because *E. albertii* is phylogenetically adjacent to but outside the *E. coli* clade (Gomes et al., 2020), I included B156 to test whether a non-*E. coli* close relative would respond differently to ARGs carriage and to, potentially, explore whether it might influence competition outcomes; as such, B156 served as an outgroup in the fitness assays.

2.1.2 ARGs

I used plasmid constructs of six ARGs, *aadA*, $bla_{TEM\text{-}116}$, $bla_{CTX\text{-}M\text{-}15}$, $bla_{SHV\text{-}12}$, *cat* and *dfrA5* from a previous study (**Table 1**). The vector plasmid (pmFP) used to construct the ARG plasmids is based on the backbone of a pUA66 plasmid without the *gfp* gene. This plasmid has Kanamycin resistance as a selection marker and the *gfp* gene has been removed to avoid any costs associated with its expression. The pUA66 plasmid, which has a pSC101 replication origin, is a low-copy-number plasmid. As it lacks the genes necessary for conjugation and an origin of

transfer, it is expected to be non-conjugative and non-mobilisable (Stirling et al., 2017; Zaslaver et al., 2006).

Table 1. ARGs used in this study

Resistance Gene	PCR Template Source	Forward and Reverse Primers	Enzyme Classification	Resistance to Antibiotics
aadA	pTargetF plasmid (Addgene, #62226)	ccgacgtctaagaaaccatgaattcctactcgagttcatgtgcagc cctcgtgatacgcctatttctgacgctcagtggaacg	Aminoglycoside O-adenyltransferase	Spectinomycin and Streptomycin
^$bla_{TEM-116*}$	portMAGE2 plasmid (Addgene, #72677)	ccgacgtctaagaaaccatgaattcttctggtcggcgcatagctg cctcgtgatacgcctattgcaagcagcagattacgcg	β -lactamase	β -lactams such as Ampicillin
bla_{SHV-12}	Based on plasmid pN18EC0432-1 GenBank: CP048293.1	ccgacgtctaagaaaccatgaattc cctcgtgatacgcctatt	β -lactamase	β -lactams like Ampicillin and Cefotaxime
$bla_{CTX-M-15}$	Based on plasmid pB20 GenBank: MK125035.1	ccgacgtctaagaaaccatgaattc cctcgtgatacgcctatt	Extended-spectrum β-lactamase	β -lactams like Ampicillin and Cefotaxime
cat	portMAGE4 plasmid (Addgene, #72679)	ccgacgtctaagaaaccatgaattcttctggtcggcgcatagctg cctcgtgatacgcctattgcaagcagcagattacgcg	Chloramphenicol acetyltransferase	Chloramphenicol
dfrA5	*E. coli* strain B706	ccgacgtctaagaaaccatgaattccatggcttgttatgactg cctcgtgatacgcctatttgtgcttagtgcatctaacg	Dihydrofolate reductase	Trimethoprim

^ The portMAGE2 encoded *BlaTEM* (*BlaTEM-116*)* differs from *BlaTEM-116* by a single amino-acid substitution at position 274.

2.2 Barcode constructs

I employed a combination of methods to facilitate the generation of barcode derivatives for each strain. This multi-stage process involves the delivery of various plasmids, each with distinct roles. For an efficient fitness-neutral delivery of the barcode cassette into the attTn7 chromosomal region of the strains, a *Tn7* helper plasmid was employed to assist the *Tn7* integration plasmid in incorporating the barcode. Subsequently, a pCP20 plasmid completes the last step of this process by facilitating Flp-catalysed excision of the antibiotic-resistance marker introduced with the barcode cassette (**Figure 1**). The resulting barcoded strains were then paired with either the vector or ARGs plasmids described in Chapter 2.1.2.

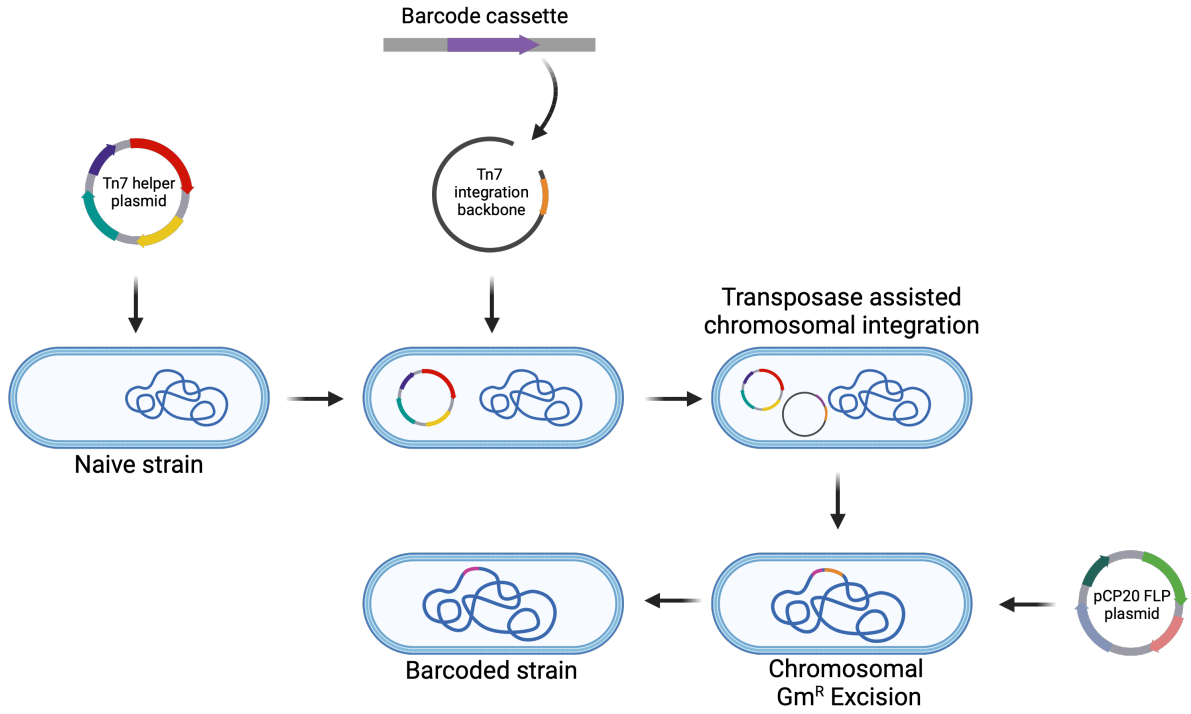

Figure 1. Overview of barcoding steps to construct the barcode libraries. First, the Tn7 helper plasmid (encoding transposase enzymes) is transformed into the naive bacterial host strain. Next, the barcode cassette is cloned into the Tn7 integration backbone plasmid, which is subsequently transformed into the strain carrying the helper plasmid. Transposase enzymes provided by the helper plasmid facilitate the site-specific integration of the barcode cassette into the bacterial chromosome. Antibiotic selection is then used to isolate successfully barcoded strains. Finally, the chromosomal antibiotic resistance marker (Gm^R) is excised using the pCP20 FLP recombinase plasmid, leaving the barcode stably integrated without the resistance gene.

2.2.1 Construction of the Tn7 integration plasmid

I constructed the Tn7 integration plasmid, pUC18R6K-mini-Tn7T-Gm-25N, using the backbone plasmid pUC18R6K-mini-Tn7T-Gm and oligonucleotides containing the 25 bp barcode. The barcode is 25 random nucleotides flanked by sequences homologous to the backbone plasmid and a NotI site. This method is further described in the next paragraph and it is based on a modified protocol used by Choi et al. on the backbone vector pUC18R6K (Choi & Schweizer, 2006) and a similar protocol used by Jasinska et al. (2020). The backbone pUC18R6K-mini-Tn7T-Gm plasmid was a gift from Herbert Schweizer (Addgene plasmid # 65022 ; http://n2t.net/addgene:65022 ; RRID:Addgene_65022). This approach resulted in a large barcode integration plasmid library, which was used to create the barcode constructs needed for this experiment.

To prepare the vector plasmids and perform transformations, I streaked colonies carrying the pUC18R6K-mini-Tn7T-Gm backbone plasmid on LB agar plates with gentamicin and incubated them at 37°C overnight. After selecting colonies, I cultured them in LB media supplemented with gentamicin (10 µg/ml). Using the Qiagen Spin Miniprep Kit, I extracted plasmid DNA, following the manufacturer's instructions, and eluted it in nuclease-free water. The plasmid concentration was measured using a Nanodrop spectrophotometer (35 ng/µl).

For PCR amplification, I used DreamTaq Green PCR master mix to amplify the extracted plasmid DNA. We prepared a 50 µl reaction mixture containing 25 µl PCR Mix (2x), 2.5 µl each of forward and reverse primers (10 µM), 2 µl plasmid DNA, and nuclease-free water up to 50 µl. The primers used in the PCR reaction are described in **Table 2,** and the primer binding sites are illustrated in **Figure 2**. We set the PCR conditions on an ABI Veriti 96 Well Thermal Cycler to an initial denaturation at 94°C for 5 minutes, followed by 25 cycles of 94°C for 20 seconds, 55°C for 30 seconds, and 72°C for 4 minutes, with a final extension at 72°C for 5 minutes.

Table 2. PCR primers used to amplify the pUC18R6K-mini-Tn7-Gm vector.

Primer Name	Primer Sequence	Primer target
581. pUC18R6K-mini-Tn7T-Gm_F	5'-CTAGCTTAATTAGCTGAGCT-3'	Amplify vector at sall cut site near Tn7R region.
582. pUC18R6K-mini-Tn7T-Gm_R	5'-CCTCGAACCCCACGCCCCTC -3'	Amplify vector at NheI cut site near Tn7R region.

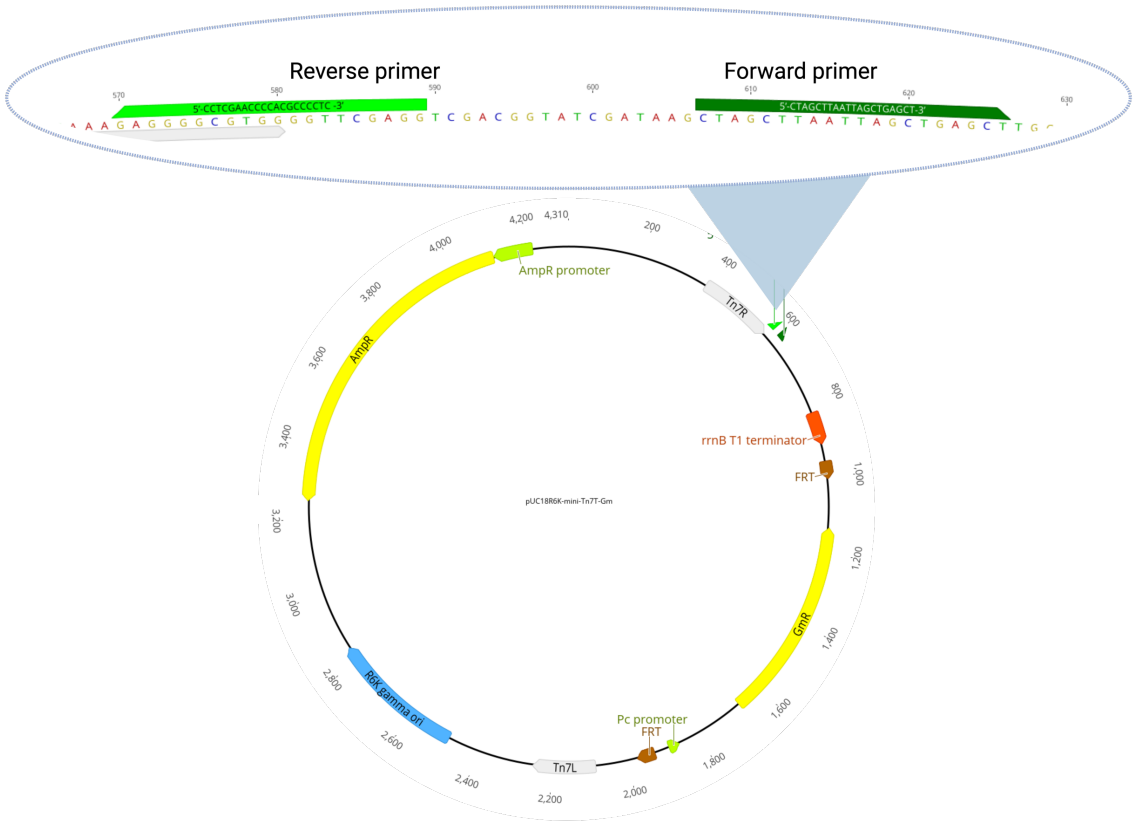

Figure 2. Primer binding sites within the barcoded integration plasmid (pUC18R6K-mini-Tn7T-Gm). The schematic illustrates the detailed binding regions of the forward and reverse primers used for barcode amplification by PCR. Primers were specifically designed to target conserved sequences flanking the barcode cassette integration site on the Tn7-based backbone. The enlarged inset clearly shows the exact nucleotide positions and orientation of primer annealing sites, facilitating targeted insertion of the barcodes.

For HiFi DNA Assembly, I used NEBuilder HiFi DNA Assembly Master Mix and followed the manufacturer's protocol, using a 5-fold molar excess of barcode oligos relative to the vector backbone. The reaction mixture included 0.033 pmol of the vector and 0.167 pmol of barcode inserts, to give a total of 0.2 pmol of DNA fragments. To remove the methylated DNA template plasmid, I performed a DpnI digest on the HiFi assembly reaction before transformations.

For electroporation, I mixed DH5α electrocompetent cells with 1 µl of the digested assembly mix and electroporated them at 1800 V, followed by recovery in SOC medium at 37°C for 1 hour. I evaluated the transformation efficiency by plating on LB agar plates containing 100 µg/mL ampicillin. To confirm the insertion of barcode oligos, I digested the extracted plasmids with NotI-HF and analysed the digested products by agarose gel electrophoresis to ensure the correct insert size. Then, I pooled colonies confirmed to have the correct plasmid insert and stored them as glycerol stocks at -80°C for long-term preservation. This formed my *Tn7* barcode integration plasmid library, which I used to barcode the attTn7 chromosomal region of the strains used in our competitions.

2.2.2 Chromosomal integration of the barcode

We used two plasmids (**Figure 3**) to insert the barcode into the chromosome: the Tn7 helper plasmid, built on the pSC101 backbone, enables site-specific integration, and the Tn7 integration plasmid described in Chapter 2.2.1, which carries the barcode cassette for integration at the attTn7 site. The construction of barcoded strains, following the method detailed here, was carried out as an equal collaborative effort with Huei-Yi Lai.
The Tn7 helper plasmid was a gift from Shimon Bershtein (Addgene plasmid # 141161 ; http://n2t.net/addgene:141161 ; RRID:Addgene_141161). The temperature-sensitive helper plasmid harbours the *tnsABCD* genes, which encode the transposase enzymatic machinery. These genes are under the control of an arabinose-inducible pBAD promoter, allowing for regulated expression of the transposase components.

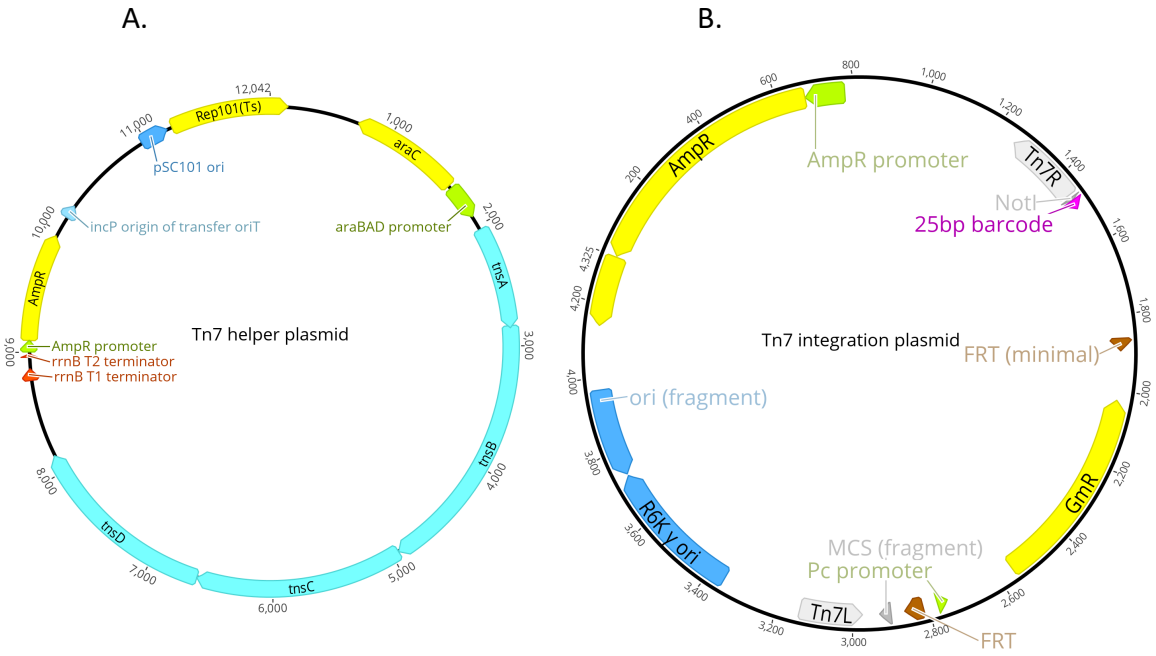

Figure 3. A. Map of the Tn7 helper plasmid showing the *tnsABCD* genes. B. Map of the *Tn7* barcode integration plasmid featuring the 25-nt barcode cassette highlighted in purple located close to the Tn7R right arm next to the NotI site.

Created using: *Geneious version 2024.0 created by Biomatters. Available from* https://www.geneious.com

Making electrocompetent bacteria cells

In this study, we chose to prepare our electrocompetent *Escherichia* cells at room temperature, a method supported by recent findings showing increased transformation efficiencies (Tu et al., 2016). This method enhances the uptake of large DNA molecules and maintains cell membrane integrity, crucial for our multiple plasmid transformations. The room temperature protocol simplifies preparation by eliminating pre-chilling, reducing procedural complexities and cellular stress. Electron microscopy shows cells prepared at room temperature retain smoother and more intact morphology, contributing to higher transformation efficiencies. This approach is cost-effective, practical, and ensures reproducibility in our experiments. Electrocompetent cells were prepared from freezer stock cultures that had been conditioned overnight. Each strain was inoculated into fresh Lysogeny Broth (LB) medium and grown to mid-exponential phase, as determined by measuring the optical density at 600 nm (OD_{600}). After reaching the desired growth phase, cells were centrifuged at 8000 rpm for 3 minutes at room temperature. The supernatant was discarded, and the cells were washed three times with sterile Mili-Q water to eliminate residual salts and media components, thereby enhancing electroporation efficiency. Finally, the cell pellet was resuspended in a minimal volume (30-40 µL) to maximize the efficiency of the transformation process. Following the first transformation and selection of cells carrying the Tn7 helper plasmid, these cells were directly used to prepare competent cells for the second transformation with the Tn7 integration plasmid.

Electroporation and Recovery

In this study, the transformation of *Escherichia* strains with the *Tn7* helper plasmid comprised the initial round of electroporation. Cultures were grown to mid-exponential phase, where the strains would reach an optical density at 600 nm (OD_{600}) between 0.400 and 0.600. For the electroporation, competent cells amounting to 50 µL were combined with 3 µL of the Tn7 helper plasmid DNA (~150 ng). The cells were allowed to sit with the plasmid DNA for 2-3 minutes before electroporation, which was performed at 1800V using a 0.1 cm gap electroporation cuvette. Following electroporation, 1 mL of warm LB without antibiotics was immediately added to the cuvette to aid cell recovery from the electric field-induced cellular damage. The recovery phase was conducted at 30°C with shaking at 200 rpm for 1 hour, followed by overnight incubation at room temperature to stabilize the transformants.

Successful transformants were selected by plating the cells on LB agar plates containing 100 µg/mL ampicillin and incubated overnight at 30°C to accommodate the temperature sensitivity of the Tn7 helper plasmid.

The second round of electroporation aimed to integrate the barcode sequence into the bacterial chromosome using the Tn7 integration plasmid. Competent cells, prepared from colonies that had successfully incorporated the Tn7 helper plasmid, were used for this transformation. These competent cells were mixed with 1 µL (267.7 ng) of the Tn7 integration plasmid DNA and electroporated using the same voltage and 0.1 cm gap electroporation cuvette. Immediately after this process, the cells were treated with 1 mL of LB, followed by an hour of recovery in similar conditions as the first round. After 45 min we added 0.2% arabinose to activate the Tn7 helper plasmid transposon machinery. Finally, to select for cells that had successfully integrated the barcode, the transformed cells were plated on LB agar containing 10 µg/mL gentamicin and incubated overnight at 30°C.

2.2.3 Selection marker excision from the chromosomal barcode cassette

The excision of the Gm resistance gene from the chromosomally integrated barcode cassette was based on the Barrick Lab protocol (Barrick et al., 2023), with modifications. The pBAD-Flp (pCP20) plasmid was a gift from Lydia Freddolino (Addgene plasmid # 122969 ; http://n2t.net/addgene:122969 ; RRID:Addgene_122969) (Scholz et al., 2019). Gm^R electrocompetent cells were transformed with the pCP20 plasmid and incubated overnight in LB + 0.2% arabinose to induce the Flp recombinase expression. The following day, we plated the transformants culture on LB + Ampicillin (100 ug/ml) selection plates and incubated overnight at 30°C. Colonies picked from these plates were inoculated into 5 ml of LB broth and incubated overnight at 43°C to select for the loss of the temperature-sensitive pCP20 plasmid. On the third day, we plated 50 µl of 10^6 dilutions of the overnight culture on LB and grew them at 30°C to avoid partial plasmid loss in colonies that have not fully lost the plasmid. The next day, we patched individual colonies from this plate onto LB + Gm, LB + Ampicillin, and LB plates in this order, ensuring LB was patched last to confirm cell transfer throughout the process. This sequence guarantees that growth on the LB plate without growth on the other plates is due to the desired phenotype and not a lack of cell transfer. We incubated the LB + Gm and LB plates overnight at 37°C, and the LB + Amp plate overnight at 30°C. We then

checked for and selected colonies that grew only on the LB plate and not on the LB + Gm or LB + Amp plates, indicating successful recombination and loss of the resistance plasmid. After the successful excision of the Gm resistance gene was confirmed by PCR, the barcoded strains were selected and sent for sequencing.

2.2.5 Construction of barcoded ARG sub-derivatives

I selected eight barcoded derivatives for each strain and paired them with the ARG plasmids detailed in Chapter 2.1.2 to create a diverse array of strain–ARG combinations. Additionally, each strain includes four barcoded vector sub-derivatives that serve as controls in the competition experiments. The ARG plasmids were introduced into each strain using the same electroporation protocol described in Section 2.2.2: cells were made electrocompetent, mixed with the plasmid DNA and electroporated. After a short recovery period in antibiotic-free medium, cells were plated onto agar supplemented with the appropriate antibiotic to select for the resistance marker carried on each plasmid, ensuring that only successful transformants formed colonies.

2.3 Plasmid loss test

In environments lacking antibiotic selection pressure, plasmid loss can occur, which can affect fitness estimates by allowing plasmid-free strains with higher fitness to dominate; thus, it is essential to investigate plasmid retention in these bacterial strains. To assess plasmid loss over time, I conducted an experiment using all six natural isolate strains containing the pmFP vector plasmid. The strains were conditioned from freezer stock by inoculating 3 ml of LB broth supplemented with 50 µg/ml kanamycin and incubated at 37°C with shaking at 200 rpm overnight. I subjected the cultures to daily 1:100 serial transfers into fresh DM250 media, inoculating 30 µl of the previous day's culture into 3 ml of fresh media, repeating this process for 7 days. On Days 0 and 7, I plated 100 µL of 10^6 dilutions of the cultures on LB agar plates to determine the total number of colonies and then transferred the colonies to selection media (LB agar plates with 50 µg/ml kanamycin) using a velvet replicator to identify plasmid-containing colonies. I quantified plasmid loss by determining the percentage of colonies that

lost the plasmid, comparing the number of colonies on selection media to the total number of colonies on LB media. The experiment was conducted in five replicates for each strain.

Plasmid loss was quantified by calculating the percentage of colonies that lost the plasmid on Day 7. This was done by subtracting the number of plasmid-containing colonies (Colonies_Selection) from the total number of colonies (Colonies_LB) and dividing by the total number of colonies, then multiplying by 100 to obtain a percentage:

$$Plasmid\ loss\ \% = \left(\frac{Colonies\_LB - Colonies\_Selection}{Colonies\_Selection}\right) \times 100$$

For statistical analysis, we performed paired t-tests to compare the total number of colonies on LB media to the number of plasmid-containing colonies on selection media for each strain. The paired t-test was chosen because it accounts for the paired nature of the observations within each replicate, thus considering replication in the analysis. The p-values obtained from the t-tests were used to assess the significance of the results, with a threshold of 0.05 set for statistical significance. Summary statistics, including the mean plasmid loss percentage and the p-values from the paired t-tests, were calculated for each strain.

2.4 Plasmid transfer test

Investigating plasmid transfer is crucial to ensure that any observed fitness effects are due to the plasmid's presence in the intended host strain and not a result of unintended plasmid acquisition by other strains, which could confound the experimental results. I conducted a plasmid transfer experiment over four days in three replicates for each bacterial strain. First, I conditioned two sets of bacterial derivatives for each strain: one set resistant to Nalidixic acid (Nx) and another set carrying the vector plasmid that confers resistance to Kanamycin (Km). On day zero, I mixed the Nx-resistant strains with the Km-resistant plasmid-mixing strains in equal amounts by measuring their optical density at OD_{600} and adjusting the cultures to the same OD_{600} value. Then, I plated the mixed cultures on three different selection media: LB+Km (50 µg/ml), LB+Nx (30 µg/ml), and LB+Km+Nx. On days zero and four, I assessed the cultures by counting colonies on each type of media. Colonies that grew on Km plates indicated the percentage of bacteria carrying the plasmid. Colonies that grew only on NX plates indicated the percentage of bacteria that did not carry the plasmid. If colonies grew on

LB+Km+Nx plates, it indicates the percentage of bacteria that had acquired the plasmid through transfer. I plated 100 µL of a 10^5 dilution on the LB+Km (50 µg/ml) and LB+NX (30 µg/ml) plates and 100 µL of a 10-fold dilution on the LB+Km+Nx plates. Finally, I recorded the number of colonies for each replicate and strain on each type of media.

2.5 Competition setup

For the competition experiments, the strains were conditioned as follows: I inoculated barcoded cells carrying the ARG plasmid from freezer stocks into 3 ml of LB broth supplemented with 50 µg/ml Km and cultured them overnight at 37°C. Then, I pre-conditioned the cultures through two 24-hour growth cycles, each consisting of a 1:100 dilution into 3 ml of fresh DM250 medium. To start the competition between multiple strains after conditioning, I combined equal volumes of the pre-conditioned cultures to create a mixed culture. For the first day of competition, we inoculated the mixed culture at a 1:100 dilution into 3 ml of DM250 in culture tubes. A 2 µL sample from the prepared mixed culture was collected for day 0 of the competition, placed in a PCR tube, mixed with 3 µL of sterile MilliQ water, and stored in the -80°C freezer until PCR amplification. The competitions were carried out for 4 days with daily 1:100 transfers into fresh medium, incubating the cultures at 37°C with shaking for 24 hours each day. Another sample was taken on the last day of the competition and stored under the same conditions. Although the data is not shown here, I compared PCR results from freshly processed samples with those stored at –80 °C and found comparable amplification and barcode recovery, indicating that freezing did not noticeably alter the results.

2.6 Competition types

To investigate the effects of ARGs on the dynamics of bacterial communities, I designed a series of competition experiments. These experiments were designed to isolate and analyse the fitness costs associated with my six focal ARGs in six host strains, and how these costs depend on community structure.

2.6.1 Competition Between a Single Strain Carrying a Single ARG (one ARG – one strain)

A single bacterial strain carrying an ARG was competed against the same strain carrying pmFP as a reference vector without the ARG. Competition was repeated for each ARG in each strain. This allows for a direct comparison of the fitness between the ARG-carrying strain and its vector-only counterpart. The primary objective of this experiment was to determine the specific fitness cost associated with carrying the ARG. By comparing the relative abundance of the strain with the ARG to that of the strain with the vector, we could assess the impact of the ARG on the growth and survival of the bacterial strain. This setup isolates the effect of the ARG, providing clear insights into its fitness cost.

2.6.2 Competition Among All Six ARGs in a Single Strain (all ARGs – one strain)

Derivatives of each bacterial strain separately carrying each of six different ARGs competed against a derivative of the same strain carrying the reference vector. Competitions were repeated for each strain. The aim of this experiment was to evaluate the relative fitness costs of different ARGs within the same genetic background. By comparing the performance of a strain with different ARGs, we could identify which ARGs impose higher or lower fitness costs. This understanding is crucial for predicting the competitive dynamics among different ARGs and their potential to persist within bacterial populations. This competition could also help us predict the dynamics in some of the other competition types.

2.6.3 Competition Among Different Strains Carrying The Same ARG (one ARG – all strains)

Multiple bacterial strains, each carrying the same ARG but differing in their genetic backgrounds, were competed against each other. The reference vector strains were also included for comparison. This experiment aimed to assess how the genetic background of the host strain influences the fitness cost of carrying the ARG. Different strains may exhibit varying levels of fitness when carrying the same ARG, highlighting the role of host background in ARG dynamics. This information is essential for understanding how ARGs might spread through diverse bacterial populations and the potential for certain genetic backgrounds to

mitigate or exacerbate the fitness cost of ARGs. This competition type could also help us predict the dynamics of the competition among all ARGs and all strains.

2.6.4 Competition Among All ARGs And All Strains (all ARGs – all strains)

All bacterial strains, each carrying one of the six different ARGs, were competed together in the same environment. Reference vector strains were included as controls. The objective of this experiment was to evaluate the overall impact of ARGs on the structure and dynamics of a complex bacterial community. By competing a diverse set of strains and ARGs together, we could observe the interactions between different ARGs and host strains, providing a holistic understanding of how ARGs influence community composition and stability. This approach offers valuable insights into the broader ecological and evolutionary consequences of ARG carriage in bacterial communities.

2.6.5 Competition Among All Strains Carrying Only The Vectors (all strains – vector)

In this setup, all six bacterial strains (H588, B354, H504, B156, M863, and REL606) carrying the reference vectors were competed against each other. This competition allows for a direct comparison of the fitness between different strains without the influence of ARGs. The primary goal of this experiment is to establish a baseline fitness for each strain when not carrying any ARGs, but when competing with other strains in the same environment. This setup serves as a control to understand how much of the fitness variation in other competitions is due to the competition between the strains versus the presence of ARGs. Additionally, it provides valuable insights into the competitive dynamics and interactions among different bacterial strains.

2.7 PCR amplification

To amplify a ~500 bp region of the target DNA, primers were designed with a melting temperature (Tm) around 60°C, minimal secondary structures, and high specificity to the target region (**Table 3**). Primers were specific to the Tn7 barcode region of the chromosome,

designed based on the sequence of the barcode cassette, making them highly conserved across all strains. PCR amplification was performed using these primers, with the bacterial culture directly as the template. This approach follows the direct PCR method as described by Song et al. (2021), which eliminates the need for time-consuming and potentially biased genomic DNA (gDNA) extraction. This method involves the use of non-ionic surfactants, such as IGEPAL CA-630, which effectively lyse bacterial cells while being compatible with PCR chemistries. This direct PCR approach was chosen due to its simplicity, cost-effectiveness, and ability to minimise biases associated with gDNA extraction. Traditional DNA extraction methods can be time-consuming, expensive, and biased based on the species present, often leading to loss of DNA during purification. Direct PCR, which skips the entire extra step of DNA extraction as it is executed within the PCR run, allows for rapid and efficient amplification directly from bacterial cultures, making it suitable for high-throughput and large-scale bacterial community analyses. This method has been shown to yield results comparable to those obtained with conventional DNA extraction kits while being significantly less expensive and faster to execute.

The PCR mix per sample was prepared as follows: 5 µL of template cultures from the competition samples stored at -80°C, 1.25 µL each of forward and reverse primers, 12.5 µL of DreamTaq Green PCR Master Mix (2X), 2.5 µL of 1% IGEPAL, and 2.5 µL of nuclease-free water, for a total volume of 25 µL. The PCR was carried out in a thermocycler with an initial denaturation at 95°C for 10 minutes, followed by 25 cycles of denaturation at 95°C for 30 seconds, annealing at 52°C for 30 seconds, and extension at 72°C for 30 seconds. A final extension was performed at 72°C for 3 minutes, followed by a hold at 4°C.

Table 3. Primers designed to amplify the 500 bp barcode region of the chromosome.

Primer Name	Primer Sequence	Primer target	Tm (melting temp)
599.Tn7_bc_7F	5'-GCGGACAATAAAGTCTTAAACTGA-3'	500 bp barcode region of the chromosome	53.3 ºC
594.Tn7_bc_655R	5'-ATCCCCAATTCGATCGTCCG-3'	500 bp barcode region of the chromosome	57.2 ºC

2.7.1 PCR clean up

To clean up the PCR products, I used Beckman Coulter AMPure XP beads. The use of AMPure XP beads at a 1.8x bead-to-sample ratio typically retains DNA fragments that are approximately 100 bp and larger, while smaller fragments such as primers, primer-dimers and unincorporated dNTPs are effectively removed (Beckman Coulter, 2023). The beads were allowed to warm up to room temperature for approximately 30 minutes. In each well of a 96-well PCR plate, I added 1.8x volumes of AMPure XP beads to 25 µL of PCR product, mixing thoroughly by pipetting up and down at least 10 times. The mixture was incubated at room temperature for 5-10 minutes to allow the DNA to bind to the beads. After incubation, I placed the plate on a magnetic stand and waited for the beads to separate, which took about 2-5 minutes until the solution became clear. The supernatant was carefully removed and discarded without disturbing the beads. I then washed the beads twice with 200 µL of freshly prepared 80% ethanol, allowing each wash to sit for 30 seconds before removing the ethanol. After the final wash, the beads were left to air-dry on the magnetic stand for 5-10 minutes. Next, I removed the plate from the magnetic stand and added 20 µL of elution buffer or nuclease-free water to each well to elute the DNA, mixing by pipetting up and down. I incubated this mixture at room temperature for 2 minutes. Finally, I placed the plate back on the magnetic stand, waited for the beads to separate, and carefully transferred the supernatant containing the cleaned PCR product to a new plate. The DNA concentration of

each sample was then measured using a double-stranded DNA (dsDNA) assay kit on a Qubit 4.0 fluorometer, preparing the samples for subsequent Oxford Nanopore Technologies (ONT) sequencing.

2.8 Oxford Nanopore sequencing

I sequenced the amplified PCR products using the ONT PromethION 2 (P2) Solo device, following the gDNA rapid barcoding protocol version **RBK_9176_V114_REVL_27NOV2022** for the sequencing library preparation. However, for amplicon DNA, I applied the recommended input quantities of approximately 50 ng per sample as specified in the **RAA_9198_V114_REVE_29NOV2023** version of the protocol. I used the new chemistry V14 with R10.4.1 flow cells, which provide superior sequencing quality and accuracy when compared to previous versions (Ni et al., 2023; Sereika et al., 2022).

2.8.1 Library preparation using Rapid Barcoding Kit 96 V14

For library preparation, I used the Rapid Barcoding Kit 96 V14 (SQK-RBK114.96) following the manufacturer's protocols. The purified PCR product for each amplicon sample was diluted to contain 50ng of amplicon DNA in 9µl of the sample and was mixed with 1 µl of rapid barcode mix. This barcoding allows for the identification of individual samples within a mixed-sample run, facilitating the multiplexing process. Once barcoding was completed, the barcoded samples were pooled together. This pool of samples underwent a second purification step using AMPure XP beads to ensure the removal of any remaining impurities that could interfere with the sequencing process. This time, I used a 1:1 ratio of beads to the sample, which is expected to retain all fragments above 300 bp and remove unincorporated rapid sequencing barcode (Beckman Coulter, 2023). The final step in the library preparation involved the ligation of sequencing adapters. These adapters are crucial because they bind the amplicons to the nanopores in the flow cell, enabling sequencing. The prepared library was stored on ice until the flow cell was ready for loading.

2.8.2 Sequencing on PromethION 2 Solo

Sequencing was performed on a PromethION 2 Solo device using PromethION Flow Cell Packs (R10.4.1). The prepared library was mixed with the sequencing buffer and library beads according to the protocol for the PromethION system. The flow cell was primed using the Flow Cell Priming Kit V14, designed to prepare the nanopore array for sequencing the prepared library. The sequencing library was then loaded onto the flow cell, taking care to avoid introducing air bubbles, which can adversely affect nanopore function and sequencing efficiency. I used MinKNOW software version 23.07.15 for real-time data acquisition during the sequencing run. Adjustments in the software settings were made to optimise the process and ensure high-quality data collection. The minimum read length was set to 200 bp, and the output file format for raw reads was set to .POD5 (4000 reads per file). On average, a full 96-sample run produced between 2.5-3 million reads. The basecalling option was turned off and was performed on the raw reads at a later stage.

2.9 Basecalling and data analysis

Soon after introducing the new chemistry in 2023, Oxford Nanopore Technologies introduced a new standalone basecalling software called Dorado (Oxford Nanopore Technologies, 2024) as part of their efforts to enhance and accelerate the basecalling processes (Oxford Nanopore Technologies, 2023). Dorado has shown significant performance improvement over its predecessor, Guppy, particularly in terms of basecalling speed and accuracy. This performance boost is largely due to Dorado's new software architecture that leverages GPUs more effectively than Guppy, which previously relied on CPUs for certain tasks (Amazon Web Services, 2023; Samarakoon et al., 2023).

2.9.1 Basecalling

Basecalling was conducted using Dorado version 0.5.3 with the model **dna_r10.4.1_e8.2_400bps_sup@v4.2.0**. This "sup" model was selected for its high accuracy, which is critical for reliable genomic analysis. The **--no-trim** argument was used to prevent

the trimming of sequencing barcodes, which are essential for the demultiplexing of pooled samples. This ensured that the entire read length was retained, preserving data integrity for comprehensive downstream analysis. The "sup" model was chosen because it offers the highest accuracy (~99.5%) among the available basecalling models. This high accuracy is crucial for accurately identifying the frequency of barcoded competitors in the samples, ensuring the reliability and quality of the sequencing data for downstream analyses.

2.9.2 Demultiplexing

Following basecalling, to accurately assign sequences to their respective samples, demultiplexing was performed using Dorado version 0.6.0. The Rapid Barcoding Kit 96 V14 (SQK-RBK114.96) was specified as an argument in the command line during the demultiplexing process to ensure the correct identification of each sample, enabling reliable downstream analyses.

2.9.3 Data analysis

Identification of Barcodes in Fastq Files

I used a custom R script to identify and count barcodes in fastq files generated from the nanopore sequencing. The script inputs the 9 base pair sequences flanking the 25 base pair barcode and employs the 'processingRawData' and 'errorCorrection' functions from the 'genBarCode' package (Thielecke et al., 2019) to identify barcode sequences within the combined set of fastq files generated for each competition. These functions accommodate up to three mismatches between target and template sequences and cluster identified barcodes with fewer than five nucleotide differences. The functions run separately to allow barcode lengths of +/-1 nucleotide from the canonical template. All resulting outputs are clustered to group identified barcodes with fewer than five nucleotide differences. This method allows computational identification of barcodes present in each competition, facilitating the detection of cross-contamination or other issues that could compromise the competition.

Counting barcode sequences

To count the occurrence of each identified barcode in each fastq file generated from a competition sample point, the 'afind' function from the 'stringdist' package was used (Loo, 2014). The 'afind' function was configured to use the 'running_cosine' fuzzy match method with stringency arguments maxdist and q.val set to 0.25 and 4, respectively. This function was also run to search for the reverse complement of each identified barcode. In rare cases where single sequences contained two identified barcodes, only one was counted. The 'afind' function was chosen due to its significantly higher count returns compared to the genBarCode functions.

Matching identified and intended input barcodes

The barcode of each host strain-plasmid resistance phenotype combination expected to be present in each competition was matched to the identified barcodes. This matching was performed using the 'afind' function, allowing up to four mismatches between intended and identified barcode sequences. Competitions were discarded from further analysis if unanticipated barcodes were identified.

Fitness estimation

Fitness was estimated by first determining the Malthusian parameter of each competitor based on the change in counts between the beginning and end of each competition. Competitions were typically conducted through four daily 1:100 transfers, estimating the Malthusian parameter as $M=\log(N_f \times 100^4/N_i)$, where N_i is the starting count for the barcode associated with a competitor and N_f is the corresponding final count. In simple terms, the equation measures how much the population has grown during the competition, considering the dilution steps, and converts this growth into a log scale for easier comparison of different growth rates. This approach assumes that overall density does not change significantly during the competition. Fitness was then estimated as the ratio of Malthusian parameters of 'test' and 'reference' genotypes. In practice, the reference Malthusian parameter was estimated as the median of all reference genotypes present in all replicates of a focal competition. In competitions containing multiple host strains, fitness was estimated separately with each host strain as the reference, allowing for comparable fitness estimates for a given host strain

in competitions when it is the only strain present against competitions where multiple strains are present.

Chapter 3: Results

3.1 No significant plasmid loss or transfer was detected

To ensure the stability of the ARG and vector plasmids in the barcoded strains, I conducted two assays: one for plasmid loss and one for potential plasmid transfer. The plasmid loss assay revealed that the mean plasmid loss percentages across the different strains ranged from 0.31% to 1.87%. Specifically, the mean plasmid loss percentages were as follows: B156 (1.16%), B354 (0.31%), H504 (1.87%), H588 (1.11%), M863 (1.21%), and REL606 (0.48%). Paired t-tests comparing the total number of colonies on LB media to the number of plasmid-containing colonies on selection media indicated that none of the strains exhibited statistically significant plasmid loss, with all p-values being well above the significance threshold of 0.05 (e.g., B156: $p = 0.208$, H504: $p = 0.070$). The plasmid loss percentages and corresponding p-values are summarised in **Table 4**. Overall, these results suggest that the vector plasmid was stably maintained across all tested strains under the experimental conditions, and plasmid loss is unlikely to affect comparisons between strains or ARGs in downstream applications.

The plasmid transfer test was conducted over four days with three replicates for each bacterial strain. Plating on selective media was used to test for plasmid transfer (details in Materials and Methods – Chapter 2.4). Importantly, no colonies were observed on LB+Km+NX plates, demonstrating the absence of plasmid transfer. The mean colony counts and standard deviations for each strain and media type are summarised in **Supplementary Table 1**. These results confirm that no plasmid transfer occurred under the experimental conditions.

Table 4. Summary of plasmid loss percentages and statistical significance across strains. This table presents the mean plasmid loss percentage for each strain after 7 days of serial transfers, along with the corresponding p-values from paired t-tests comparing the total number of colonies on LB media to the number of plasmid-containing colonies on selection media.

Strain	Mean Plasmid Loss Percentage (%)	p-value	95% CI
B156	1.16	0.208	[-0.51, 1.71]
B354	0.31	0.374	[-0.36, 0.76]
H504	1.87	0.070	[-0.08, 1.28]
H588	1.11	0.374	[-0.71, 1.51]
M863	1.21	0.374	[-0.71, 1.51]
REL606	0.48	0.374	[-0.36, 0.76]

3.2 Processing barcode sequencing data and evaluating barcode fidelity

After verifying that plasmid loss and transfer were negligible, the next step was to evaluate the nanopore sequencing reads to quantify barcode frequencies and calculate fitness. For each competition experiment, the 25-bp chromosomal barcode of each strain was PCR amplified and sequenced on an Oxford Nanopore platform as described in the Materials and methods section. A custom R script scanned the FASTQ reads for the constant primer sequences flanking the barcode and extracted the intervening barcode sequence; reads lacking these flanking sequences or containing ambiguous bases were discarded. To give a sense of scale, an illustrative competition generated 21 833 raw reads, of which 9 796 reads (~45 %) contained an identifiable barcode; the remaining reads were filtered out because the barcode region was absent or unrecognisable due to sequencing errors. These proportions are typical of the competitions reported in this thesis. Once barcodes were extracted, reads were grouped by barcode sequence and counted. Counts at the beginning and end of each competition were converted to relative frequencies to calculate the fold-change of each lineage; relative fitness estimates were then obtained by comparing the fold-changes of ARG-carrying strains to those of control strains as described later in Chapter 3.

When barcode reads were analysed, up to four mismatches between an observed barcode sequence and its corresponding reference were allowed. To assess whether this mismatch criterion led to loss of data, the example dataset was reprocessed using a more permissive threshold of five mismatches: only 10 additional barcodes were recovered (9 796 → 9 806), indicating that the four-mismatch criterion did not appreciably reduce the number of barcodes detected. It is important to note that there is no objective way to determine the total number of barcodes that could be found, because the denominator depends on how divergent a sequence must be to be called a barcode. The approach described here therefore balances the need to capture genuine barcodes against the risk of inflating barcode counts with sequencing errors and provides a transparent account of how raw sequencing data are converted to the quantitative fitness values.

3.3 Comparison of the fluorescent marker and barcode frequency methods for estimating ARG fitness effects

To comprehensively evaluate the fitness effects of antibiotic resistance genes (ARGs) in bacterial populations, it is essential to compare different methodologies. This comparison aims to assess the consistency and reliability of fitness estimates obtained through two different approaches: the fluorescent marker method used in a separate study (Lai & Cooper, 2024) and the barcode frequency method employed in this study.

The fitness estimates obtained by our lab in a different study using the fluorescent marker approach were compared with those derived from the barcode frequency approach. The overall correlation between the two sets of estimates is very low ($r = 0.01$, $P = 0.95$), which is likely due to the relatively low signal in the data relative to the noise. This is particularly evident when comparing fitness estimates per ARG (**Figure 4**), where differences across the approaches are generally low compared to the error.

To better understand the differences between fitness estimate approaches, I used ANOVA, comparing models with and without the competition method as a factor. In both models, the ARG-by-strain interaction was included as a random effect to account for variation in fitness estimates associated with specific ARG and strain combinations, regardless of the measurement method. I found a significant effect of the approach used ($\chi^2 = 14.31$, $P > 0.001$). This indicates that while the two methods do not correlate, they systematically differ in how they estimate fitness. It is also worth noting that fitness estimates from the barcode method appear more tightly clustered together, suggesting a greater sensitivity and lower variability compared to the fluorescent marker method, which shows more dispersed fitness estimates (**Figure 4**).

The significant ANOVA result suggests that the choice of method matters and may introduce systematic differences in fitness estimates. Further data will be required to determine whether these differences stem from methodological biases or biological factors affecting competition outcomes.

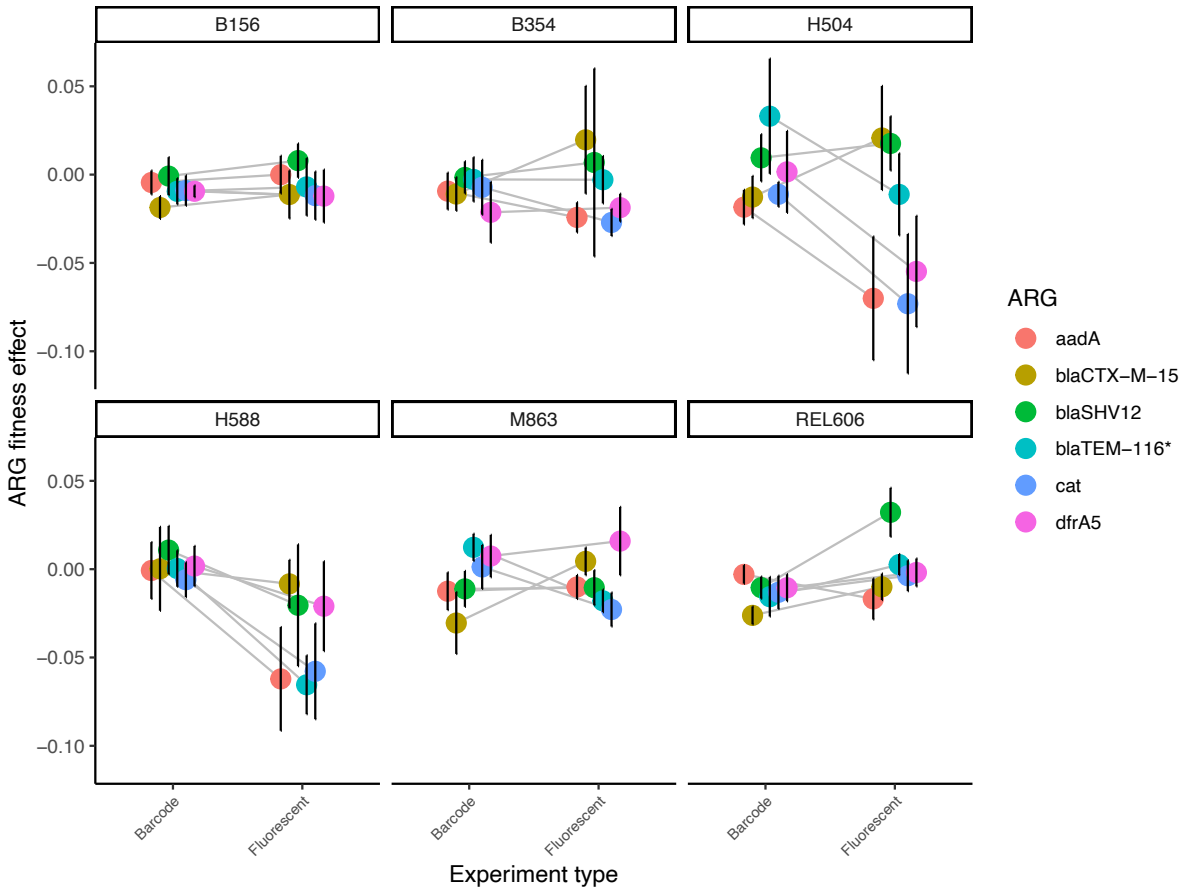

Figure 4. Comparison of fitness estimates for ARGs using fluorescent marker and barcode frequency methods. Fitness estimates of ARGs using the fluorescent marker and barcode frequency methods across six bacterial strains. Lines connect fitness estimates for the same ARG, with error bars representing standard errors. Replication: n>12 – fluorescent marker method and n>10 – barcode frequency method.

3.4 Fitness effects of ARGs

To understand how ARGs affect the fitness of host bacteria, I need to isolate the fitness cost or potential benefit associated with a single ARG in a specific bacterial strain. I do this by comparing a strain carrying an ARG encoded on a vector to the same strain carrying only the vector, allowing me to precisely quantify the fitness cost imposed by the ARG. This direct comparison is essential for understanding the fundamental costs of ARG carriage without the confounding effects of interactions with other genes or strains. The competition between a single strain carrying an ARG and its Vector allows for a controlled and straightforward analysis of the fitness costs associated with individual ARGs when in specific bacterial strains.

3.4.1 ARGs impose costs on their hosts in environments without selection pressure from antibiotics.

To quantify the fitness costs imposed by ARGs, I calculated the relative fitness of each ARG across the six bacterial strains used in this work. I found that ARGs had significant effects on host fitness (comparison of ANOVA models with and without the ARG term χ^2= 16.03, $p < 0.001$). To avoid the risk of false positives that could result from multiple comparisons, I used the Willcoxon test with Benjamini-Hochberg (BH) correction when comparing the overall fitness costs of ARGs to the vector (**Figure 5)**. This test revealed four of the six tested ARGs (*aad*, *bla*$_{CTX\text{-}M\text{-}15}$*, cat, dfrA5)* imposed a significant fitness cost ($p<0.05$); **Table 5**. However, Willcoxon test combines data across all strains and may not reflect strain-specific effects.

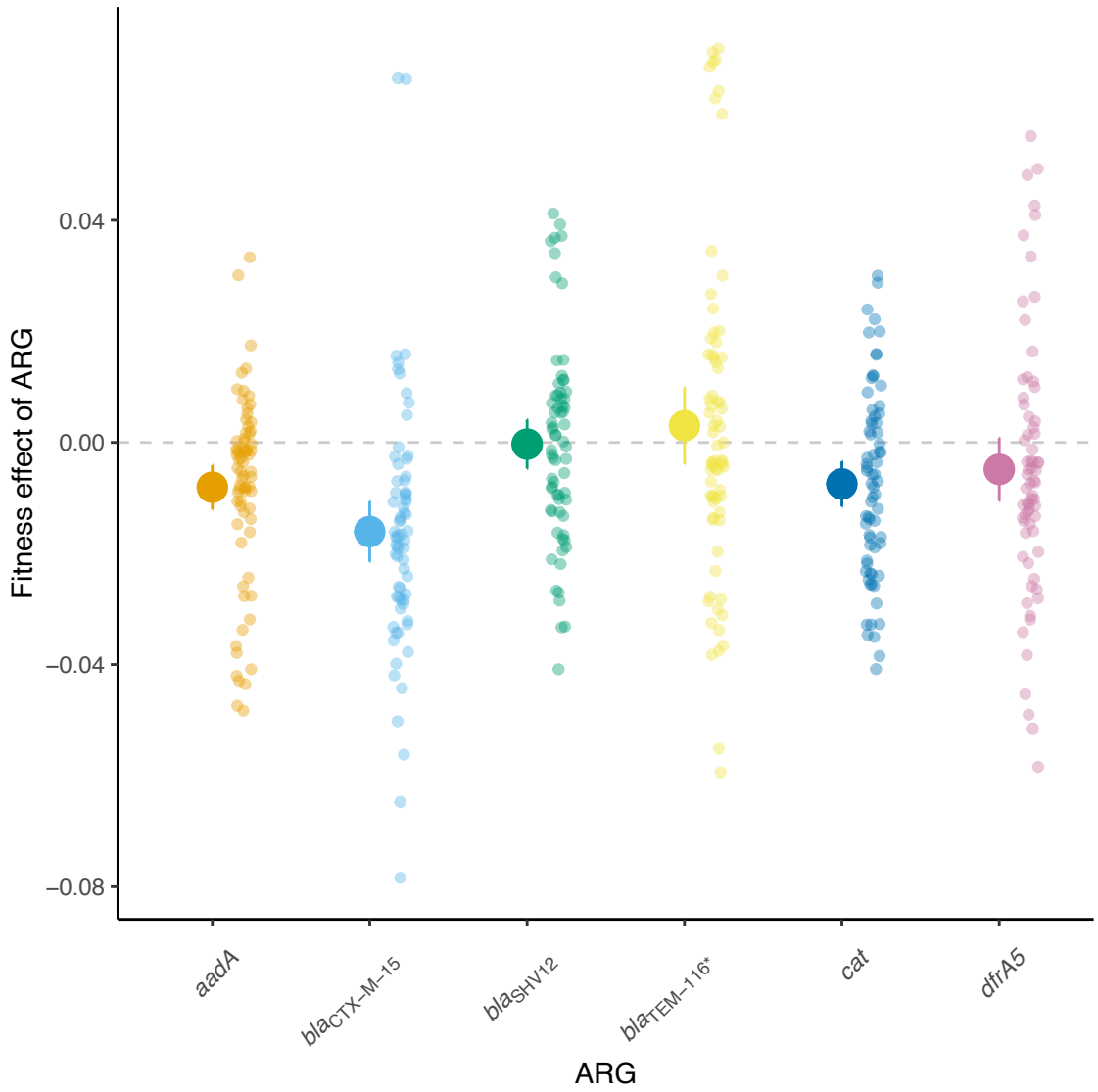

Figure 5. Mean fitness effects of ARGs compared to the vector control. Fitness effects of ARGs relative to the vector across all strains. Large symbols indicate the mean, error bars represent 95% confidence intervals and small symbols represent individual fitness measurements of the indicated ARG across all tested host strains. At least 68 independent fitness estimates were used for each ARG.

Table 5. Mean fitness effects of ARGs compared to vector. Summary statistics from Dunnett's test, which was used to compare the fitness effects of each ARG against a vector control across all six bacterial strains. Dunnett's test was used to compare the mean fitness effect of each ARG against the vector control across all strains, which provided a single, multiple-comparison-corrected test to determine which ARGs imposed a fitness cost relative to the control. The raw p-values were adjusted using the Benjamini-Hochberg (BH) correction to control for the false discovery rate. Asterisks indicate the level of statistical significance for the ARGs with statistically significant results (*>0.05, **>0.01, ***>0.001, ****>0.0001).

ARG	Vector (n=381)	ARG Sample Size	Raw *p*-value	Adjusted *p*-value (BH)	Significance
aadA	vs.	72	<0.001	<0.001	***
$bla_{CTX\text{-}M\text{-}15}$	vs.	70	<0.001	<0.001	***
bla_{SHV12}	vs.	68	0.654	0.785	ns
$bla_{TEM\text{-}116*}$	vs.	72	0.891	0.891	ns
cat	vs.	70	<0.001	<0.001	***
dfrA5	vs.	69	<0.001	0.001	**

3.4.2 Fitness effects are strain dependent.

It is important to determine whether the effect of ARGs varies across different bacterial strains to help us determine whether host genetic backgrounds can affect the persistence and spread of resistance. For example, it is possible that some strains act as cost-free 'reservoirs' that allow the maintenance of ARGs even in the absence of antibiotic pressure. This knowledge is useful for predicting resistance dynamics and informing targeted interventions to combat antibiotic resistance.

To investigate the strain-dependent fitness effects of ARGs, I considered fitness estimates of all ARGs separated by the host strain. I found strong support for differences in the mean fitness effect of ARGs between different host strains (comparison of models with and without ARG-by-strain term: $\chi^2 = 19.13$, $p < 0.001$; **Figure 6**). Dunnett's test reveals that all ARGs except *aadA* have a significant fitness effect in at least one strain (**Supplementary Table 2**). All fitness effects were negative except a noticeable beneficial 3.3% increase in fitness conferred by $bla_{TEM\text{-}116*}$ in the H504 strain (**Figure 7**). By contrast, $bla_{TEM\text{-}116*}$ imposed costs on other strains like REL606 and B156. $bla_{CTX\text{-}M\text{-}15}$ imposed significant fitness costs in in REL606, B156, and M863 ($p < 0.001$), while *dfrA* was costly in REL606, B156, and B354. Among the host strains analysed, all except H588 showed significant fitness changes linked to at least one ARG ($p<0.05$). In the strain REL606, five out of the six ARGs tested imposed significant fitness costs.

3.4.3 Fitness variation is driven by ARG-strain interactions in pairwise competitions.

To fully understand and quantify the relative variance of the factors that contribute to the fitness effects observed, I analysed the contribution of each term to the random-effect model. Strain accounted for 2.34% (+/- 1.7% 95%CI) of the total variance in ARG fitness effects, explaining the smallest proportion of variance. This small strain effect suggests that even if some strains may be better or worse at carrying some of the ARGs, this is not necessarily the main determinant of fitness variation in my results. By contrast, ARGs account for 5.35% (+/- 2.2% 95%CI) of the total variance. This means that some of the ARGs impose larger fitness effects regardless of the host strain. While this explains the variance more than the strains do, it is still a relatively small percentage, confirming that no single ARG affects every host

tested. More significant is the interaction between ARG and strain, which explains 13.18% (+/- 1.8% 95%CI) of the variance. This percentage of the variance is larger than either individual term alone, suggesting that the fitness impact of an ARG is dependent on the strain that carries it. Instead of an ARG being costly or beneficial in all host strains, its fitness effects can change from detrimental in some strains to neutral or even beneficial in others. This finding shows how the largest random variance in fitness is not driven by a specific ARG or strain alone, but rather by the interaction between the two. The remaining portion of the variation reflects unexplained residuals, primarily due to variation between experimental replicates.

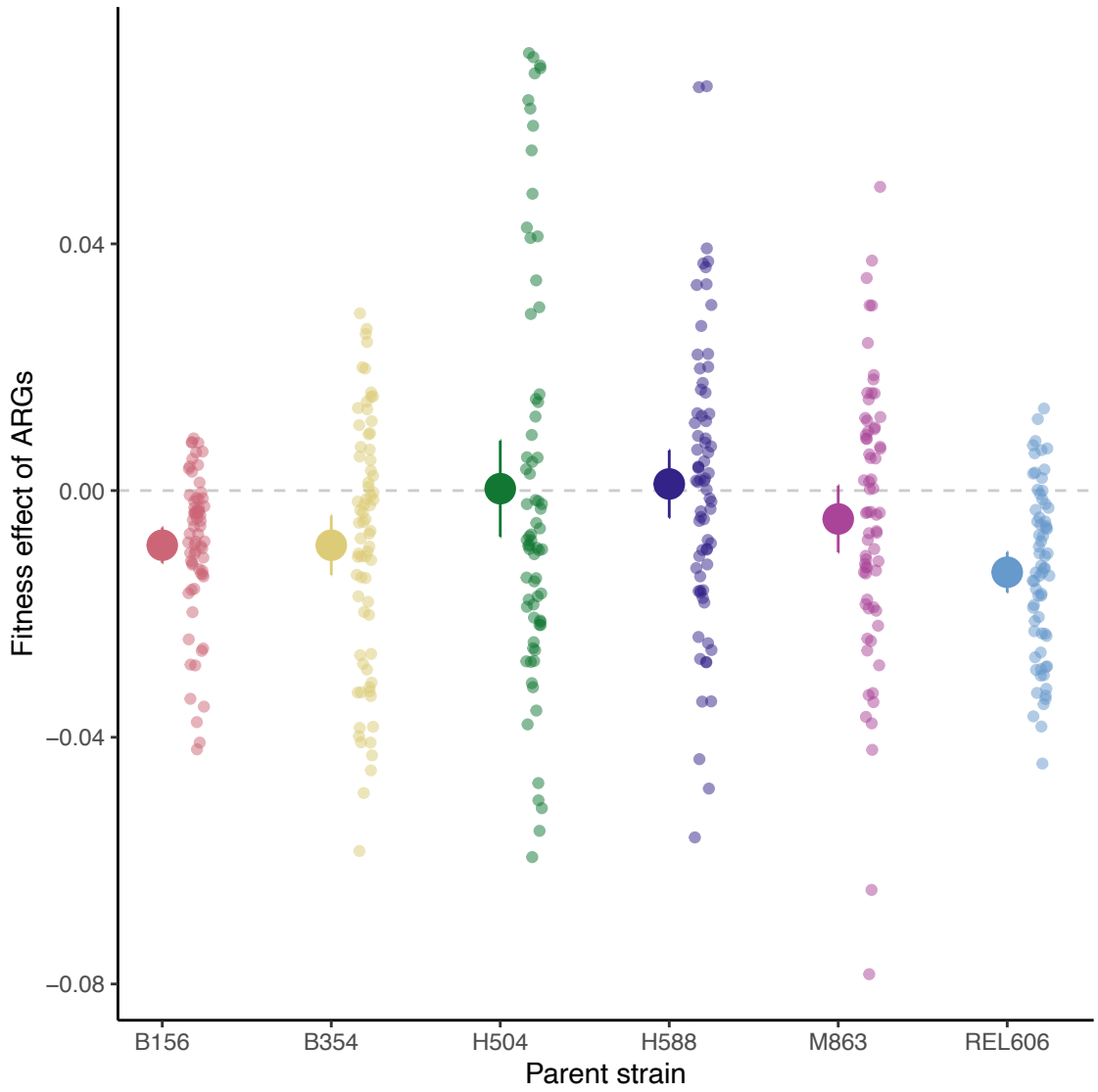

Figure 6. Mean fitness effects of ARGs in each strain. Fitness effects of ARGs relative to the vector in each strain. Large symbols indicate the mean, error bars represent 95% confidence intervals and small symbols represent individual fitness measurements of the indicated host strain across all tested ARGs. At least 68 independent fitness estimates were used for each host strain.

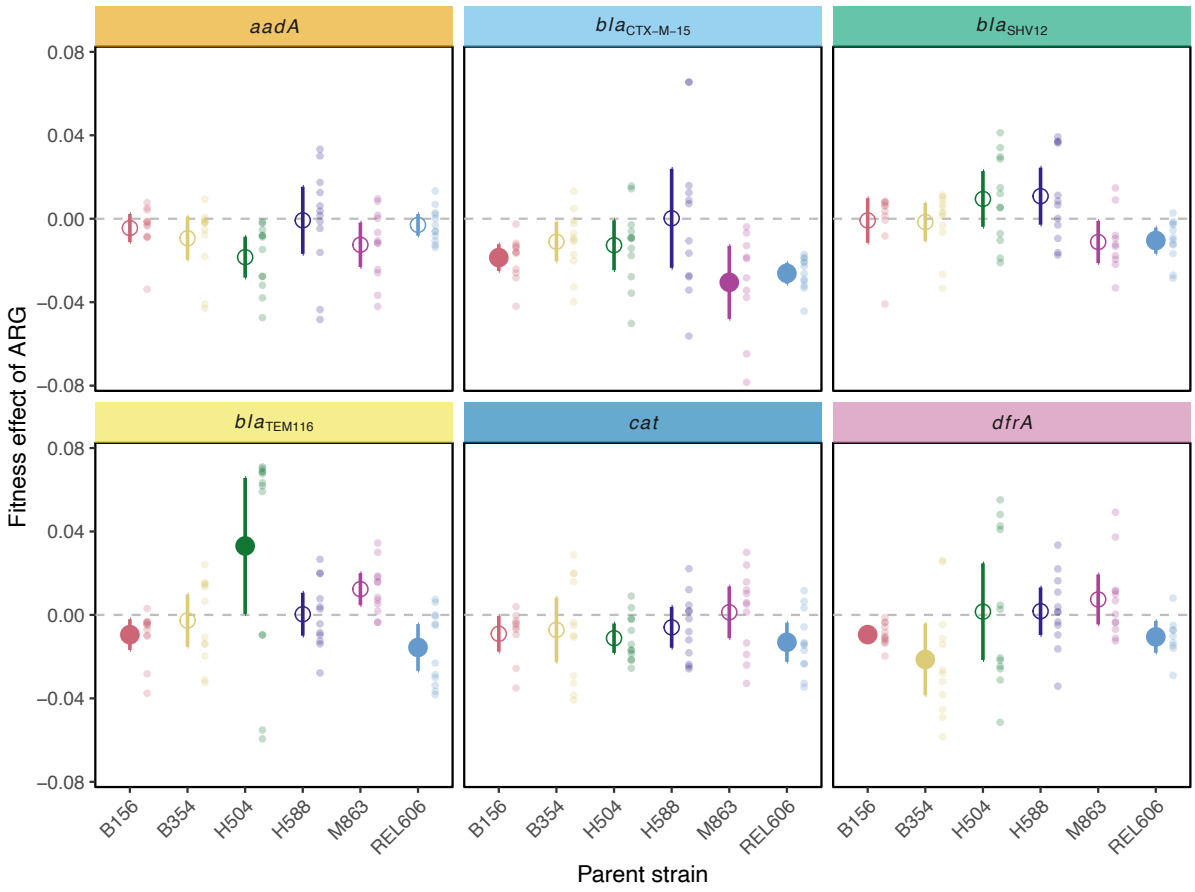

Figure 7. Fitness effect of each ARG in each strain. Fitness effect of each ARG relative to the vector in each strain. Large symbols indicate the mean, error bars represent 95% confidence intervals and small symbols represent individual fitness measurements of the effect of each ARG on each of the six host strains. The filled large symbols represent significant ARG effects from Dunnett's test ($p < 0.05$). At least nine replicates for each independent ARG-strain combination were used for these measurements.

3.5 Community composition affects the cost of resistance.

To investigate how the competition context influences the fitness effects associated with ARGs I compared the data obtained from four competition designs: (i) **one ARG – one strain (1ARG-1S)**, (ii) **all ARGs – one strain (allARG-1S)**, (iii) **one ARG – all strains (1ARG-allS)**, and (iv) **all ARGs – all strains (allARG-allS)**. These competition types are described in more detail in Chapter 2.6. Comparing these results enabled me to quantify the influence of community composition on the outcomes of competitions from three aspects: the effect of ARGs, host strain fitness, and the interaction between ARGs and strains.

3.5.1 The fitness effects of ARGs depend on the specific competition environment.

To fully understand ARG effects across different competition contexts, I first assessed the cost of each ARG compared to the reference vector within the same strain in different competition types (**Table 6 –** summarises only ARGs found to show significant differences between competition types). While the competition type alone did not have any overall effect on ARG fitness, I found a significant effect that depended on the interaction between ARG and competition type (ARG-by-competition type effect: χ^2 = 41.8, P < 0.001; **Figure 8**). This suggests that the fitness effects of ARGs depend on the specific competition environment.

For example, *bla*$_{TEM\text{-}116*}$ gene has conferred a slight fitness increase of 0.3% (+/- 0.7% 95%CI) in the '1ARG-1S' competition but imposed a significant cost of 3.1% (+/- 1.5% 95%CI) in the 'allARG-allS' competition. More interestingly, the *bla*$_{CTX\text{-}M\text{-}15}$ gene had a relative fitness cost of 1.6% (+/- 0.5% 95%CI) in the '1ARG-1S' competition, but this dropped to only 0.6% (+/- 0.4% 95%CI) in 'allARG-1S' competition. The *bla*$_{SHV12}$ gene shows a clear shift in fitness effects between different competition types, displaying an almost neutral effect of 0.03% (+/- 0.4% 95%CI) in the '1ARG-1S' competition, but in the one '1ARG-allS' competition it imposes a cost of 1.9% (+/- 1.0% 95%CI) and further decreases fitness by 2.4% (+/- 1.3% 95%CI) in all 'allARG-allS' competitions. All test comparisons between different competition types for each ARG are summarised in the **Supplementary Table 3**.

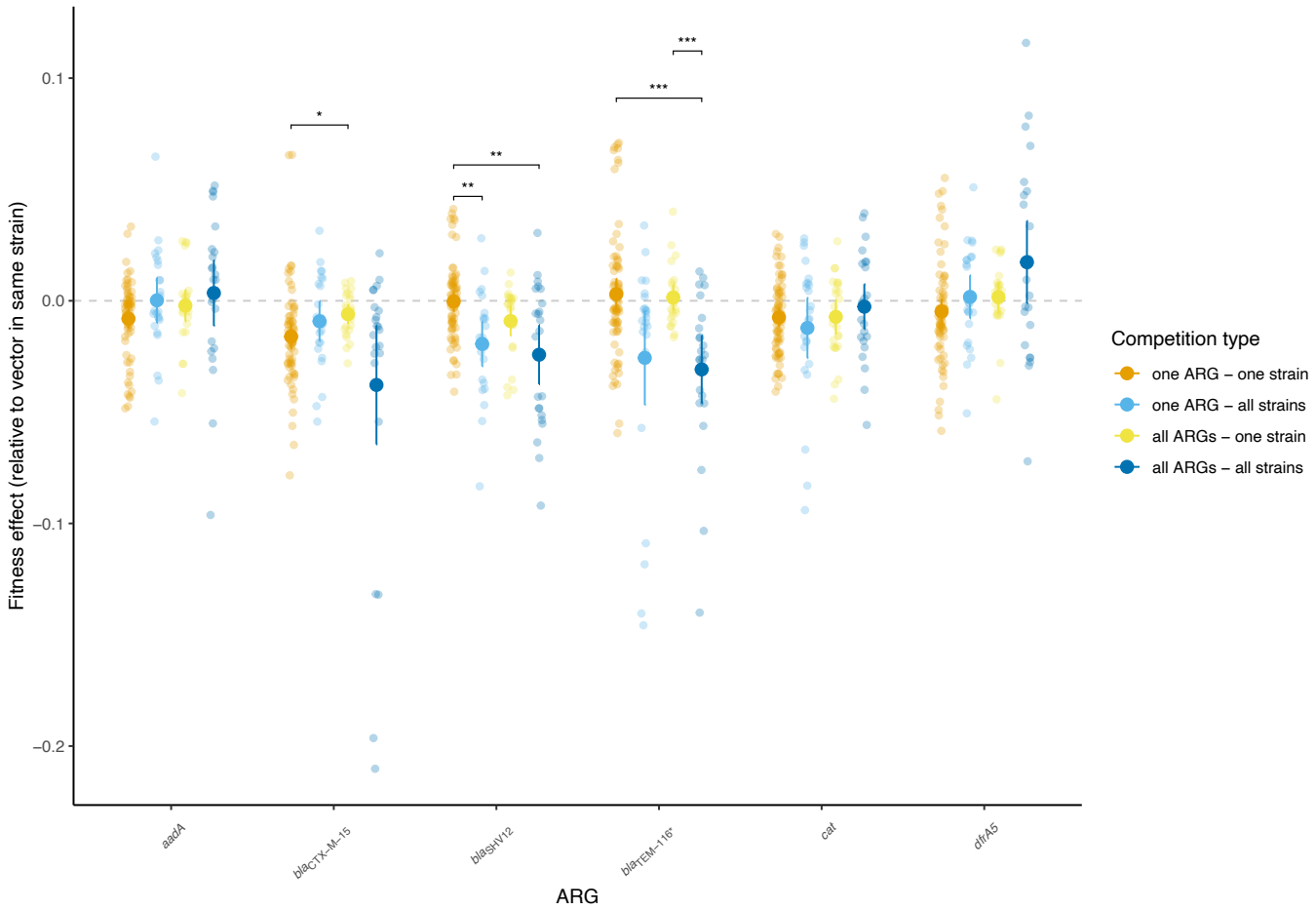

Figure 8. Fitness effect of each ARG across all strains in different competition types. Mean fitness effect of each ARG, indicated on the x-axis, in all strains relative to the vector in the same strain and competition type. Large symbols indicate the mean fitness effect, error bars represent 95% confidence intervals and small symbols represent individual fitness estimates. Asterisks represent significant differences between competition types for each ARG (Wilcoxon test with BH correction for multiple tests within each group; *>0.05, **>0.01, ***>0.001, ****>0.0001). At least 24 replicates for each ARG-competition type interaction were used to determine fitness effects.

Table 6. Summary of fitness effects of ARGs in different competition environments. Summary statistics representing the relative fitness effects of ARGs under different competition types, showing only results where statistically significant interactions are present. The relative fitness effect and confidence intervals are presented in percentages (%), and to further illustrate the precision of these estimates, the number of replicates for each treatment type is shown.

Competition type	ARG	Relative fitness effect (%)	Replication	CI (%)
one ARG – one strain	*bla*$_{CTX\text{-}M\text{-}15}$	-1.6	70	0.5
one ARG – all strains	*bla*$_{CTX\text{-}M\text{-}15}$	-0.9	24	0.9
all ARGs – one strain	*bla*$_{CTX\text{-}M\text{-}15}$	-0.6	24	0.4
all ARGs – all strains	*bla*$_{CTX\text{-}M\text{-}15}$	-3.8	24	2.7
one ARG – one strain	*bla*$_{SHV12}$	-0.03	68	0.4
one ARG – all strains	*bla*$_{SHV12}$	-1.9	24	1.0
all ARGs – one strain	*bla*$_{SHV12}$	-0.9	24	0.7
all ARGs – all strains	*bla*$_{SHV12}$	-2.4	24	1.3
one ARG – one strain	*bla*$_{TEM\text{-}116*}$	0.3	72	0.7
one ARG – all strains	*bla*$_{TEM\text{-}116*}$	-2.6	24	2.1
all ARGs – one strain	*bla*$_{TEM\text{-}116*}$	0.2	24	0.6
all ARGs – all strains	*bla*$_{TEM\text{-}116*}$	-3.1	24	1.5

3.5.2 The fitness effects of ARGs depend on the host strain and vary across different competition types.

Next, I determined if the fitness effects of ARGs varied depending on the host strain across the different competition types. The competition type alone did not have an overall effect on the strain fitness; however, it did have an effect dependent on the strain, as indicated by a significant strain-by-competition type interaction (χ^2 = 169.6, P < 0.001; **Figure 9**). This suggests that ARGs can have different fitness effects depending on the host strain and competition type. For example, the effect of ARGs on strain B156 fitness was 0.9% (+/- 0.3% 95%CI) in '1ARG-1S' competitions but increased to 3% (+/- 1.1% 95%CI) in 'allARG-allS' competitions (**Figure 9**). I observed an even stronger effect of ARGs on the REL606 strain fitness, from a negative 1.3% (+/- 0.3% 95%CI) across the '1ARG-1S' competitions to an even larger negative effect of 5.9% (+/- 2.9%) in the 'allARG-allS' competition. Interestingly, the effect of ARGs on strains B354 and H588 was positive when going from simpler competitions to more complex competition environments, suggesting an advantage for these strains in more complex competition environments. For example, the effect of ARGs on B354 strain conferred a slight fitness improvement of 1.8% (+/- 1.5% 95%CI) in 'allARG-allS' competition, despite showing a 0.9% (+/- 0.5% 95%CI) fitness reduction in the '1ARG-1S' competitions. Similarly, strain H588 showed a 1% (+/- 0.3% 95%CI) fitness reduction in '1ARG-allS' competitions but it showed a 0.2% (+/- 0.5% 95%CI) increase in 'allARG-allS' competition, suggesting a slight advantage when multiple ARGs are present. All statistically significant results of the effects of ARGs on host fitness, in different competition types, are summarised in **Table 7.** All test comparisons between different competition types for each strain are summarised in the **Supplementary Table 4**.

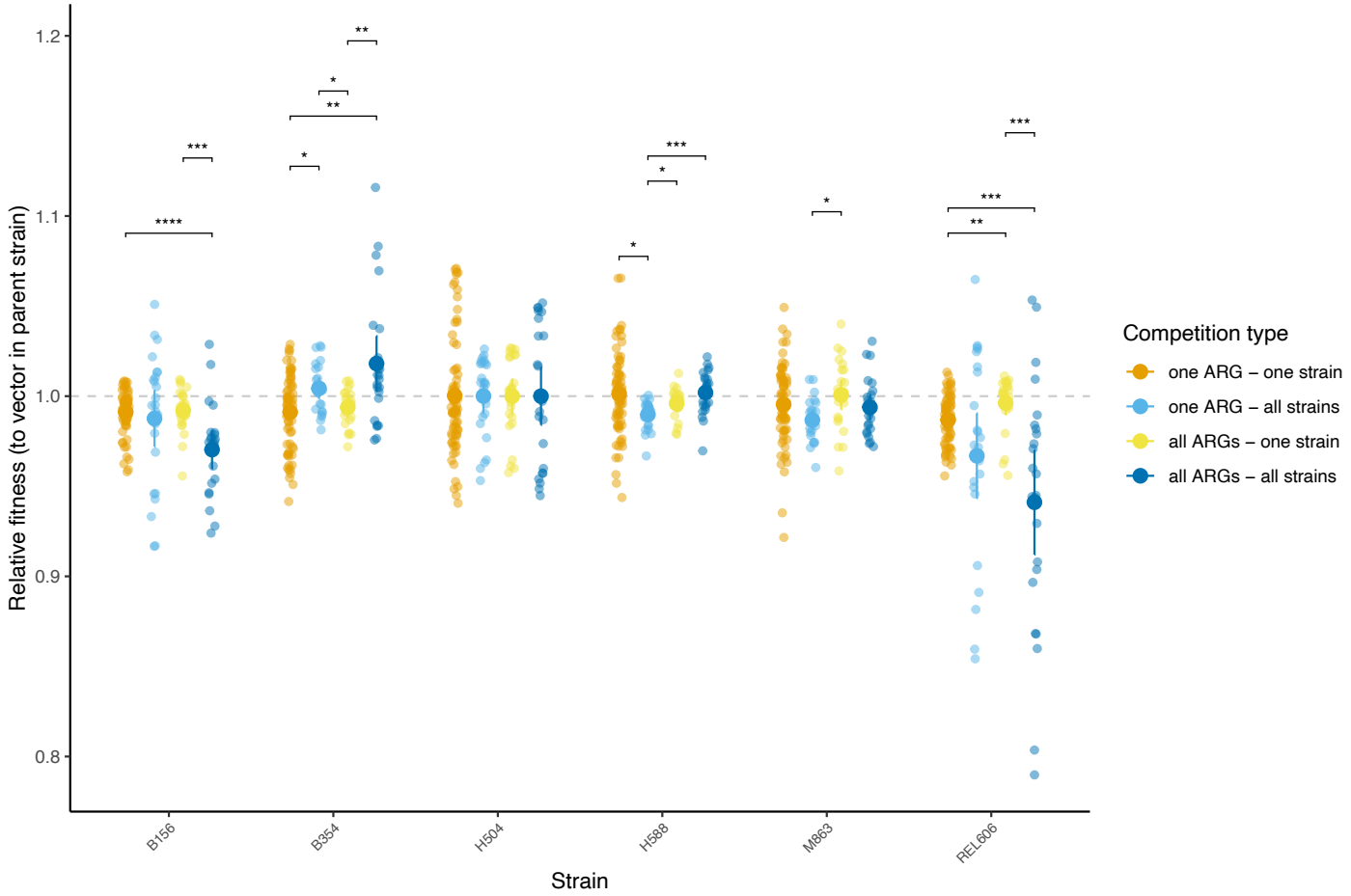

Figure 9. ARGs effect on strains across different competition types. Mean fitness effect of ARGs relative to the vector in the same strain and competition type. Large symbols indicate the mean fitness effect, error bars represent 95% confidence intervals and small symbols represent individual fitness estimates. Asterisks represent significant differences between competition types for each ARG (Wilcoxon test with BH correction for multiple tests within each group; *>0.05, **>0.01, ***>0.001, ****>0.0001). At least 24 replicates for each strain-competition type interaction were used to determine the fitness effect.

Table 7. Summary of host strain fitness effects in different competition environments. Summary statistics representing the relative fitness effects on host strains across different competition types, showing only results where statistically significant interactions are present. The relative fitness effects and confidence intervals are presented in percentages, and to further illustrate the precision of these estimates, the number of replicates for each treatment type is shown. H504 not shown since no significant strain-dependent effects were observed across different competition types.

Competition type	Parent Strain	Relative fitness effect (%)	Replication	CI (%)
one ARG – one strain	B156	-0.9	68	0.3
one ARG – one strain	B354	-0.9	72	0.5
one ARG – one strain	H588	0.1	72	0.5
one ARG – one strain	M863	-0.5	68	0.5
one ARG – one strain	REL606	-1.3	69	0.3
one ARG – all strains	B156	-1.2	24	1.6
one ARG – all strains	B354	0.4	24	0.6
one ARG – all strains	H588	-1.0	24	0.3
one ARG – all strains	M863	-1.3	24	0.5
one ARG – all strains	REL606	-3.3	24	2.4
all ARGs – one strain	B156	-0.8	24	0.5
all ARGs – one strain	B354	-0.6	24	0.4
all ARGs – one strain	H588	-0.4	24	0.3
all ARGs – one strain	M863	0.1	24	0.8
all ARGs – one strain	REL606	-0.4	24	0.6
all ARGs – all strains	B156	-3.0	24	1.0
all ARGs – all strains	B354	1.8	24	1.5

all ARGs – all strains	H588	0.2	24	0.5
all ARGs – all strains	M863	-0.6	24	0.7
all ARGs – all strains	REL606	-5.9	24	2.9

3.5.3 ARG fitness effects are shaped by strain identity and competition type.

Considering the combined effects of ARGs, strains and competition types, I found a highly significant three-way interaction (χ^2 = 151.8, P < 0.001). While some strains may gain a competitive advantage in more complex competition environments (B354), others (REL606 and B156) can incur significant fitness reductions in these environments (**Figure 10**). This indicates that the fitness effects of ARGs are highly strain-dependent and influenced by the community context in which these strains and ARGs are present.

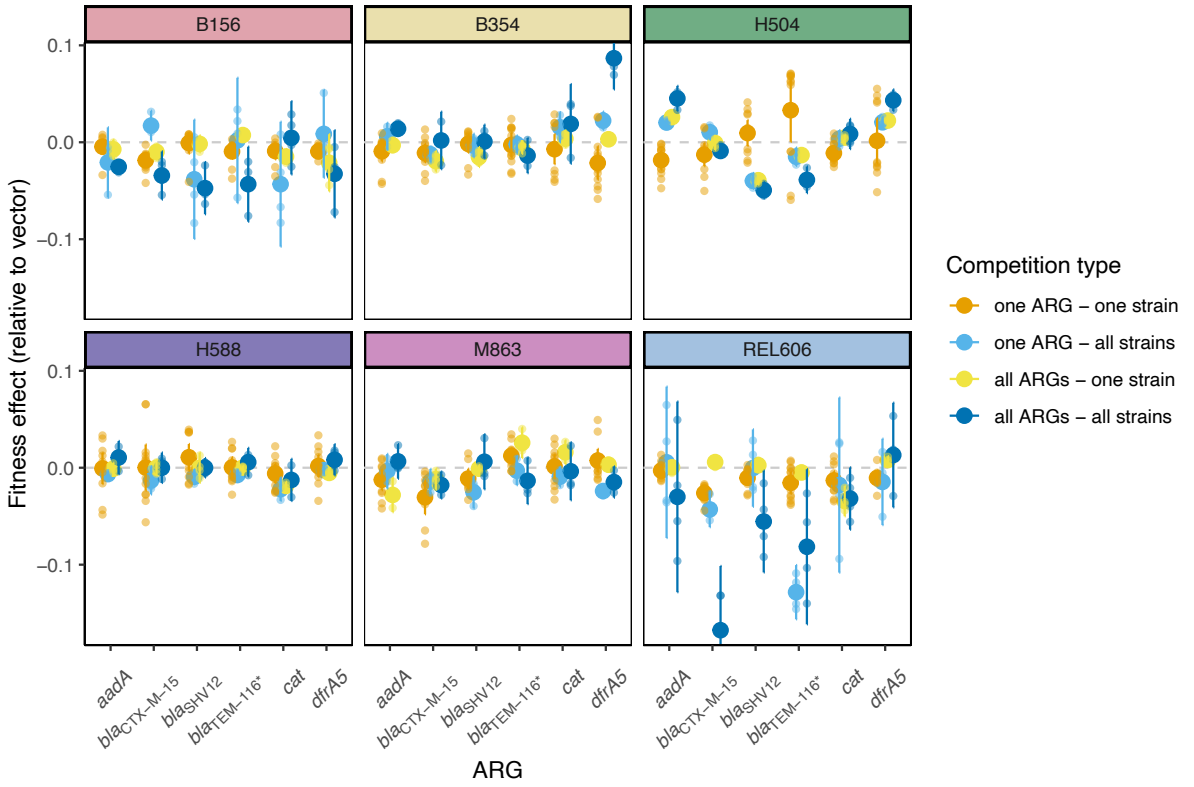

Figure 10. Mean fitness effects of ARGs relative to vector controls across different competition types and host strains. Large symbols represent mean fitness effects, error bars indicate 95% confidence intervals, and small symbols depict individual fitness measurements for each ARG within the indicated host strain and competition type. Each ARG-strain-competition type combination includes at least 4 independent fitness estimates.

Chapter 4: Discussion

My findings reveal that the fitness costs associated with ARGs are highly context-dependent, varying with both the host bacterial strain and the surrounding community. In monoculture experiments, several ARGs imposed a detectable fitness burden on their hosts in the absence of antibiotic selection, consistent with the notion that expressing resistance can be costly (Hernando-Amado et al., 2017). In fact, four of the six tested ARGs conferred a significant overall fitness cost across all host backgrounds in our study **(Figure 5)**, underscoring that many resistance elements do carry a net burden when antibiotics are absent. However, these costs were not uniform: ARGs effect ranged from being negligible in some of the host strains to being significantly costly or even beneficial in others **(Supplementary Table 2)**. Conversely, each host strain suffered a fitness reduction from at least one of the ARGs. This host-specific pattern means that certain ARG–host combinations act as "selective refuges," allowing the ARG to persist with little cost in those genetic backgrounds. In turn, these strains can act as ARG reservoirs for these genes and have a significant impact on the spread of resistance (Carrera Páez et al., 2024; von Wintersdorff et al., 2016).

4.1 Strain-specific fitness effects

A key finding of this study is that the host genetic background plays an important role in determining ARG fitness costs. The effect of a given ARG varied dramatically across the six *Escherichia* strains tested (Chapter 3.4.2), indicating a significant strain-by-ARG interaction. Many resistance genes that were costly in one strain were nearly neutral – or even beneficial – in others. For example, $bla_{TEM\text{-}116^*}$ provided a ~3% fitness boost to strain H504, yet the **same gene** imposed a fitness cost in strains REL606 and B156. Likewise, the extended-spectrum β-lactamase $bla_{CTX\text{-}M\text{-}15}$ imposed significant fitness reductions in the strains REL606, B156, and M863 ($p < 0.001$ in each case) but had negligible impact on the other three strains tested. Interestingly, our lab strain REL606 was the most strongly affected by five out of six ARGs, contrasting to strain H588, which was not statistically affected by any ARG. These results demonstrate that fitness effects are highly strain-dependent. The same ARG can be a considerable burden in one genome and nearly invisible in another. This finding is consistent

with prior research showing that plasmid-borne traits (including antibiotic resistance) often have variable fitness outcomes in different bacterial backgrounds (Humphrey et al., 2012).

The fitness impact of a given ARG can differ dramatically depending on the host strain that carries it. In other words, what is costly in one strain may be relatively benign in another. Comparative studies have shown that the same resistance gene or plasmid can incur a very different fitness cost across different host strains (Vogwill & MacLean, 2015). A meta-analysis examining dozens of plasmid experiments revealed that the fitness effects of an individual plasmid varied just as much across different hosts as entirely distinct plasmids did within a single host. This means one cannot reliably extrapolate the cost of an ARG from one strain to another – each host-ARG combination is unique (Humphrey et al., 2012). For example, as early as 2007, De Gelder et al. (2007) observed that a broad-host-range plasmid was maintained in some *E. coli* lineages but rapidly lost in others, indicating that host genetics determined whether the plasmid's fitness effect led to long-term persistence or plasmid loss. Similarly, Humphrey et al. (2012) reported that *E. coli* harbouring the same IncP-1 resistance plasmid showed different fitness outcomes: some strain backgrounds tolerated the plasmid with minimal cost, while others experienced significant growth reductions. These findings highlight that the fitness cost of an ARG is not fixed or inherent but depends heavily on the host's genetic background.

4.2 Community context determines the success of ARGs and strains.

The results presented in the analysis above reveal that the impact of ARGs on the bacterial fitness is not fixed and it varies between different competition environments. Some strains, such as B156 and REL606, incurred greater costs when all ARGs were introduced in the multi-strain competitions ('allARG–allS') compared to simpler ones ('1ARG-1S'). These larger costs led to disadvantages for these strains in the more complex competitive environments. By contrast, other strains (e.g., B354, H588) maintained or improved their relative fitness despite the increase in the number of ARGs or strains present, suggesting that these strains are capable of compensating and tolerating the burden imposed by ARGs more effectively.

These differences in competitive outcomes suggest that whether an ARG is lost or maintained does not depend only on its own fitness effect in a particular strain but also on the capacity of that strain to compete against other community members carrying different ARGs. Therefore, community context – both in terms of the number of strains and types of ARGs they harbour – can change which strains thrive and whether an ARG persists.

4.3 Strains, ARGs and the community context

When all the factors – ARG identity, host strain, and community context – are considered together, the picture that emerges is one of **highly specific interactions**. My experiments testing ARG effects across multiple competition types revealed a significant three-way interaction (ARG × strain × competition environment; Section 3.5.3). This means that the fitness effect of a given ARG cannot be generalised without specifying **both** the host and the environment; the three factors together determine the outcome. Perhaps the most striking evidence for this was seen in the **multi-strain community competitions** (Section 3.5), where each strain carrying a different ARG competed simultaneously in the all 'ARGs-allS' competition type. In this scenario, the **community context ultimately determined the "winners"** and **"losers"** in ways that were not predictable by looking at single-strain competitions alone.

The fitness costs of ARGs observed in simple competitions may be amplified or offset when strains compete within more complex competitions. For example, strain B156 experiences only a minor cost from ARG carriage in a simple one-on-one competition (~0.9% fitness reduction in the '1ARG – 1S' context), but when all ARGs and all strains were together, B156's average cost increased to about 3%. An even more dramatic case is the lab strain REL606: it had a ~1.3% overall fitness cost from ARGs in the simplest competitions, yet in the six-strain competition, REL606's fitness declined to nearly −6% on average. In other words, REL606 carrying various ARGs was severely outcompeted when placed in a diverse community. These higher fitness costs in complex environments translated into clear competitive disadvantages. By contrast, other strains performed much better as the competition environment became more complex. Strain B354 is a good example: it showed a modest cost (~0.9% fitness

reduction) in the simple competitions, but in the all strains community, B354 actually achieved a slight fitness advantage (about +1.8%). Similarly, strain H588 went from a small cost (~−1% in a '1ARG – allS' context) to essentially no cost or a slight benefit (+0.2%) in the full community competition. In practical terms, B354 and H588 were among the "winners" of the multi-strain competition – they maintained or increased their population shares despite each carrying an ARG, whereas REL606 and B156 were "overwhelmed" by the combined burden of their ARGs and the strong competition from other strains.

The multi-strain competition experiments point to something that previous single-strain or pairwise studies could easily miss. If one were to examine these ARGs only in isolation, one might conclude (correctly) that some have mild costs and one even has a benefit in a particular host. But when all six ARGs and six strains were put together, the **evolutionary outcome** (which ARGs and strains persist) was not fully predictable from the isolated measurements. For instance, $bla_{CTX\text{-}M\text{-}15}$ appeared very costly in REL606 alone, yet in the community context, REL606 incurred substantial fitness costs regardless of which ARG it carried (**Figure 7**) – the strain's inherent competitive inferiority "decided" its fate, illustrating that the availability of competitor strains can determine which ARG is ultimately maintained. Likewise, the presence of strains like H588 that can tolerate ARGs means those ARGs are more likely to stick around in the community, even if other strains would pay high costs for them. In summary, the interplay between **which strains are present** and **which ARGs they carry** is crucial in shaping community composition over time. My findings thus provide experimental support for the idea that neither plasmid cost nor host fitness alone can predict ARG dynamics – we must consider the full **ARG–host–community triangle**.

These outcomes indicate that the capacity of a strain to compete against others can amplify or compensate for the effect of its own ARG cost, depending on the community context. A strain that is inherently a poor competitor will be hit twice as hard if it also carries a costly resistance gene, especially in the presence of other, more competitive strains. On the other hand, a highly competitive strain can sometimes overcome even a moderate fitness cost of an ARG, leveraging its competitive advantage to offset the burden.

4.4 Extension beyond ARGs: Costs of accessory gene expression in the mobile plasmidome

The strain- and community-dependent fitness effects observed for ARGs likely generalise to many other genes carried on mobile plasmids. Plasmids often harbour diverse accessory traits beyond antibiotic resistance – including virulence factors, heavy metal and toxin resistances, metabolic pathways, and symbiotic functions – that can similarly alter host fitness in context-specific ways (Hall et al., 2015; Wardell et al., 2022). For example, pheromone-responsive plasmids in Enterococcus can transfer not only ARGs but also virulence genes between strains (García-Solache & Rice, 2019). Likewise, some plasmids carry toxin-antitoxin systems or bacteriocin genes; these ensure plasmid maintenance by killing plasmid-free segregants, but improper expression (e.g. toxin without antitoxin) can severely inhibit host growth (Gerdes et al., 1986; Qi et al., 2021). Each of these non-ARG traits may impose a baseline metabolic burden on the host, yet confer crucial advantages under specific environmental or community conditions.

Heavy metal resistance plasmids provide a clear parallel to ARGs: they can be costly to maintain in metal-free conditions but hugely beneficial when metals are present. In Pseudomonas fluorescens, carriage of mercury-resistance plasmids had strongly context-dependent fitness effects, acting as a growth handicap in the absence of mercury but turning into a net benefit under high mercury levels (Hall et al., 2015). In mixed soil communities, the otherwise outcompeted P. fluorescens strain was able to persist when carrying a mercury-resistance plasmid in mercury-polluted soil, whereas plasmid-free cells were driven below detectable levels – demonstrating how plasmid-borne traits can rescue a host's competitiveness in a community when environmental conditions favour that trait (Hall et al., 2020). Such traits can alter microbial community structure by enabling plasmid-bearing populations to flourish on otherwise unusable resources, thereby reshaping competition and resource partitioning.

Plasmid-encoded virulence factors in pathogens follow the same pattern. They are often indispensable for causing disease in a host organism, yet they may carry significant fitness

costs in the absence of that host or when expressed at high levels. For instance, the virulence (Ti) plasmid of Agrobacterium tumefaciens imposes almost no cost when simply maintained, but expressing its infection genes is energetically very expensive (Platt et al., 2012). In plant infection experiments, Agrobacterium strains carrying the virulence plasmid could successfully induce tumours and access nutrients, but "cheater" bacteria that had lost the plasmid still benefited from those nutrients without paying the plasmid's expression cost. As a result, the competitive outcome between virulent (plasmid-bearing) and non-virulent (plasmid-free) strains depended on environmental context – the presence of susceptible plant hosts and the availability of resources released by infected plants. This example underscores that plasmid advantages and costs are highly conditional. When conditions induce the plasmid-encoded trait (e.g. host-derived signals triggering virulence gene expression), the plasmid-bearing strain pays a high price, which can be exploited by competitors. On the other hand, when the benefits of carrying a plasmid exceed the associated costs (such as access to host nutrients or defence against antibiotics/heavy metals), plasmids will have a clear competitive advantage.

Equally important to how accessory gene plasmids shape microbial communities as they evolve over time are the community interactions of the host strains. A given plasmid's fitness impact can vary dramatically across different bacterial hosts (Alonso-del Valle et al., 2021), meaning that the success of a plasmid-borne gene (and the frequency of that gene in a community) is determined by the host species or strain carrying it. Studies have found that even broadly transmissible plasmids do not affect each host equally – some hosts incur heavy burdens while others experience minimal cost or even net gain from the same plasmid (Alonso-del Valle et al., 2021; Humphrey et al., 2012). This variability influences which host lineages maintain the plasmid in a mixed community, thereby affecting community composition. For example, plasmids in rhizobia that carry symbiotic nitrogen-fixation genes (necessary for plant root nodulation) tend to persist only in hosts that engage in the legume symbiosis; in non-symbiotic hosts those large plasmids are often lost unless they also carry additional benefits (Wardell et al., 2022). Indeed, losing such symbiosis plasmids can reduce a bacterium's competitive fitness – rhizobial strains without their sym-plasmid often lose traits like certain metabolic capabilities or bacteriocin production(Hirsch, 1979; Oresnik et al., 2000), making them less competitive in the soil ecosystem (diCenzo et al., 2014). By linking

multiple beneficial functions on one mobile element, plasmids can ensure their stability and spread: bacteria that acquire a plasmid gain a suite of adaptive traits (antibiotic and heavy metal resistance, virulence factors, resource utilisation enzymes, etc.), which can be essential for survival in complex communities. In turn, the distribution of these traits across microbial populations is heavily influenced by the ecological context. Environmental pressures select for bacteria with plasmids carrying the relevant adaptive genes, which alters community structure by favouring those plasmid-bearing subpopulations. As populations evolve, plasmids can drive niche differentiation by conferring bacteria with different accessory genes depending on their environment and competitors. This process ultimately shapes diverse microbial communities adapted to certain ecological contexts.

In summary, the finding that ARG fitness costs depend on host background and community context is one example of a broader principle shaping the plasmidome. Mobile plasmids collectively act as a dynamic reservoir of adaptive functions, and the fitness effects of expressing any given plasmid-encoded gene (be it an ARG, a virulence determinant, a catabolic enzyme, or a stress resistance factor) are context-dependent. These context-specific costs and benefits mean that plasmid-borne genes will spread or be maintained only under certain ecological conditions (Alonso-del Valle et al., 2021; Platt et al., 2012). When those conditions are met – for example, the presence of antibiotics, heavy metals, a favourable host, or a particular nutrient – plasmid carriers gain an advantage that can change competitive landscapes and restructure the community. However, in permissive environments without those pressures, plasmid-bearing cells are often outcompeted by plasmid-free counterparts due to the burden of carrying and expressing extra genes (De Gelder et al., 2007; Hall et al., 2015). The evolutionary and ecological impact of the plasmidome, therefore, lies in this interplay between genetic context and environment. By transferring a wide array of accessory genes, plasmids continuously promote adaptation and influence which bacteria thrive in a given community, ultimately shaping microbial community structure and function in every ecosystem where they are found.

4.5 Future research and conclusion

Finally, I note several **open questions for future research**. One key question is **identifying the genetic determinants** that make one host a low-cost carrier and another host a high-cost carrier of the same plasmid. Is it differences in specific regulatory genes, metabolic capacity, or something like plasmid copy number control? Advances in genomics could allow us to pinpoint these factors by comparing strains. Another open area is to explore how **community complexity** beyond a few species influences plasmid dynamics – most experiments (including mine) use relatively simple communities, but natural environments have hundreds of species. Do my findings scale to those complex ecosystems, or do new emergent behaviours appear when there are many potential hosts and interactions? Additionally, while I have extended the argument beyond ARGs conceptually, more work is needed on **other plasmid-encoded traits** in diverse hosts to see if their cost-benefit dynamics shape community structure in a similar way. For example, do plasmids carrying biodegradation pathways or heavy metal resistance follow the same rules of host-dependent fitness effects and community-dependent maintenance? Early evidence and theory suggest yes, since the "plasmid paradox" of why costly plasmids persist applies broadly (Carroll & Wong, 2018), but solid experimental demonstrations in environmental contexts would be valuable.

In conclusion, my discussion illustrates that the persistence and evolution of ARG-bearing plasmids (or other accessory genes) are driven by a complex interplay of host-specific factors, community interactions, and evolutionary adaptations. The findings in my study can be linked to broader biological concepts: host-specific costs (Chapter 3.4) mean plasmids will selectively thrive in compatible hosts (Vogwill & MacLean, 2015); community context (Chapter 3.5) can either accelerate plasmid loss through competition or facilitate retention (Kottara et al., 2021; Sünderhauf et al., 2023); and over time, plasmid-host systems may evolve towards equilibrium via compensation (Harrison et al., 2015) or gene integration events (Bergstrom et al., 2000), ultimately shaping which genes remain mobile in a community. My results, placed in context with recent studies, reinforce a view of plasmids as **dynamic players in microbial ecosystems** – not static genetic elements but ones whose success depends on the ecological context and evolutionary adaptations. This has important implications for understanding and managing antibiotic resistance spread, and it suggests that reducing the burden of ARGs in

clinics or the environment will require strategies that consider the **genetics of hosts (to possibly increase costs), the structure of communities (to prevent easy refuge or transfer), and the capacity for evolutionary change (to avoid rapid compensation)**. By considering my experimental findings with contemporary research, I conclude that combating ARG plasmids is as much an ecological and evolutionary challenge as it is a pharmacological one. The plasmidome's future will be shaped by how these factors play out, and this study provides some insight towards understanding and influencing that outcome.

Supplementary data

Supplementary Table 1. Summary statistics of colony counts in plasmid transfer assay.

The "Strain" column specifies the bacterial host strain tested. "Media" indicates the selection media type:

- **LB+Km (50 µg/ml):** Selects for plasmid-containing strains (kanamycin resistance).
- **LB+NX (30 µg/ml):** Selects for plasmid-free strains (nalidixic acid resistance).
- **LB+Km+NX:** Dual-antibiotic media is used to detect plasmid transfer (no growth is expected if no plasmid transfer was detected).

"Mean" represents the average colony-forming units (CFU) across six experimental replicates. "SD" denotes the standard deviation of colony counts, reflecting biological variability. "n" indicates the total number of replicates (n=3 replicates per strain/day combination).

Strain	Media	Day	Mean colonies	SD	n
B156	LB+Km	Day 0	219	5.13	3
B156	LB+Km	Day 4	207	3.06	3
B156	LB+NX	Day 0	208	5.51	3
B156	LB+NX	Day 4	222	15.6	3
B156	LB+Km+NX	Day 0	0	0	3
B156	LB+Km+NX	Day 4	0	0	3
B354	LB+Km	Day 0	219	8.33	3
B354	LB+Km	Day 4	226	13.1	3
B354	LB+NX	Day 0	228	3.06	3
B354	LB+NX	Day 4	219	21	3
B354	LB+Km+NX	Day 0	0	0	3
B354	LB+Km+NX	Day 4	0	0	3
H504	LB+Km	Day 0	213	7.55	3
H504	LB+Km	Day 4	215	17	3
H504	LB+NX	Day 0	223	12.1	3
H504	LB+NX	Day 4	225	13.9	3
H504	LB+Km+NX	Day 0	0	0	3
H504	LB+Km+NX	Day 4	0	0	3
H588	LB+Km	Day 0	217	3.61	3
H588	LB+Km	Day 4	238	6.24	3

H588	LB+NX	Day 0	221	6.24	3
H588	LB+NX	Day 4	221	13.7	3
H588	LB+Km+NX	Day 0	0	0	3
H588	LB+Km+NX	Day 4	0	0	3
M863	LB+Km	Day 0	207	3	3
M863	LB+Km	Day 4	207	7.57	3
M863	LB+NX	Day 0	225	6.51	3
M863	LB+NX	Day 4	222	16.6	3
M863	LB+Km+NX	Day 0	0	0	3
M863	LB+Km+NX	Day 4	0	0	3
REL606	LB+Km	Day 0	222	4.62	3
REL606	LB+Km	Day 4	226	6.56	3
REL606	LB+NX	Day 0	202	2.65	3
REL606	LB+NX	Day 4	202	3.51	3
REL606	LB+Km+NX	Day 0	0	0	3
REL606	LB+Km+NX	Day 4	0	0	3

Supplementary Table 2. Dunnett's Test Results for the Fitness Effects of ARGs Relative to the Vector Control. The "ARG" column indicates the antibiotic resistance gene being tested, and the "Strain" column specifies the bacterial strain in which the ARG was evaluated. "Estimate" represents the mean difference in relative fitness (r.ref) between the ARG and vector control. Negative values indicate a fitness cost, while positive values suggest a potential fitness advantage. "SE" (standard error) provides a measure of variability around the estimate. "t-value" represents the test statistic assessing the strength of the difference between the ARG and vector. "p-value" indicates the probability of observing the result under the null hypothesis, and "Significance" denotes the adjusted p-value after Dunnett's correction for multiple comparisons. Asterisks indicate the level of statistical significance for the ARGs in the tested strain (*>0.05, **>0.01, ***>0.001, ****>0.0001).

ARG	Strain	Estimate	SE	t-value	*p*-value	Significance
aadA	REL606	−0.003	0.0029	−1.01	0.889	ns
	B156	−0.004	0.0035	−1.28	0.727	ns
	B354	−0.009	0.0045	−2.06	0.218	ns
	H504	−0.018	0.0090	−2.04	0.211	ns
	H588	−0.001	0.0056	−0.14	1.000	ns
	M863	−0.012	0.0062	−2.00	0.247	ns
$bla_{CTX\text{-}M\text{-}15}$	REL606	−0.026	0.0029	−8.89	<0.001	***
	B156	−0.019	0.0035	−5.35	<0.001	***
	B354	−0.011	0.0045	−2.42	0.094	ns
	H504	−0.013	0.0090	−1.41	0.596	ns
	H588	+0.0002	0.0056	+0.04	1.000	ns
	M863	−0.030	0.0068	−4.51	<0.001	***
bla_{SHV12}	REL606	−0.010	0.0029	−3.55	0.003	**
	B156	−0.001	0.0038	−0.22	1.000	ns
	B354	−0.002	0.0045	−0.35	0.999	ns
	H504	+0.009	0.0090	+1.05	0.837	ns
	H588	+0.011	0.0056	+1.94	0.278	ns
	M863	−0.011	0.0068	−1.65	0.459	ns
$bla_{TEM\text{-}116*}$	REL606	−0.016	0.0029	−5.30	<0.001	***
	B156	−0.009	0.0035	−2.72	0.043	*
	B354	−0.003	0.0045	−0.60	0.990	ns

	H504	+0.033	0.0090	+3.66	0.002	**†
	H588	+0.0004	0.0056	+0.06	1.000	ns
	M863	+0.012	0.0062	+1.98	0.256	ns
cat	REL606	−0.013	0.0029	−4.45	<0.001	***
	B156	−0.009	0.0038	−2.40	0.100	ns
	B354	−0.007	0.0045	−1.58	0.512	ns
	H504	−0.011	0.0090	−1.23	0.720	ns
	H588	−0.006	0.0056	−1.07	0.859	ns
	M863	+0.001	0.0062	+0.20	1.000	ns
dfrA5	REL606	−0.011	0.0033	−3.16	0.012	*
	B156	−0.009	0.0035	−2.71	0.044	*
	B354	−0.021	0.0045	−4.70	<0.001	***
	H504	+0.002	0.0090	+0.17	1.000	ns
	H588	+0.002	0.0056	+0.32	1.000	ns
	M863	+0.007	0.0062	+1.19	0.788	ns

Supplementary Table 3. Wilcoxon test comparison between competition types for each ARG (BH correction). The "ARG" column indicates the antibiotic resistance gene being tested, and the "Competition type x" column specifies the competition group compared. nX represents the number of replicates for each competition type. The raw p-values were adjusted using the Benjamini-Hochberg (BH) correction to control for the false discovery rate. Asterisks indicate the level of statistical significance for the ARGs between the competition types tested (*>0.05, **>0.01, ***>0.001, ****>0.0001).

ARG	Competition type 1	Competition type 2	n1	n2	Adjusted *p*-value (BH)	Significance
aadA	one ARG - one strain	one ARG - all strains	72	24	0.393	
aadA	one ARG - one strain	all ARGs - one strain	72	24	0.393	
aadA	one ARG - one strain	all ARGs - all strains	72	24	0.06	
aadA	one ARG - all strains	all ARGs - one strain	24	24	1	
aadA	one ARG - all strains	all ARGs - all strains	24	24	0.461	
aadA	all ARGs - one strain	all ARGs - all strains	24	24	0.393	
$bla_{CTX\text{-}M\text{-}15}$	one ARG - one strain	one ARG - all strains	70	24	0.152	
$bla_{CTX\text{-}M\text{-}15}$	one ARG - one strain	all ARGs - one strain	70	24	0.012	*
$bla_{CTX\text{-}M\text{-}15}$	one ARG - one strain	all ARGs - all strains	70	24	0.921	
$bla_{CTX\text{-}M\text{-}15}$	one ARG - all strains	all ARGs - one strain	24	24	0.865	
$bla_{CTX\text{-}M\text{-}15}$	one ARG - all strains	all ARGs - all strains	24	24	0.188	
$bla_{CTX\text{-}M\text{-}15}$	all ARGs - one strain	all ARGs - all strains	24	24	0.118	
bla_{SHV12}	one ARG - one strain	one ARG - all strains	68	24	0.003	**
bla_{SHV12}	one ARG - one strain	all ARGs - one strain	68	24	0.112	
bla_{SHV12}	one ARG - one strain	all ARGs - all strains	68	24	0.007	**
bla_{SHV12}	one ARG - all strains	all ARGs - one strain	24	24	0.112	
bla_{SHV12}	one ARG - all strains	all ARGs - all strains	24	24	0.814	
bla_{SHV12}	all ARGs - one strain	all ARGs - all strains	24	24	0.112	
$bla_{TEM\text{-}116*}$	one ARG - one strain	one ARG - all strains	72	24	0.053	
$bla_{TEM\text{-}116*}$	one ARG - one strain	all ARGs - one strain	72	24	0.936	
$bla_{TEM\text{-}116*}$	one ARG - one strain	all ARGs - all strains	72	24	0.000221	***
$bla_{TEM\text{-}116*}$	one ARG - all strains	all ARGs - one strain	24	24	0.053	

bla$_{TEM-116*}$	one ARG - all strains	all ARGs - all strains	24	24	0.117	
bla$_{TEM-116*}$	all ARGs - one strain	all ARGs - all strains	24	24	0.000221	***
cat	one ARG - one strain	one ARG - all strains	70	24	0.976	
cat	one ARG - one strain	all ARGs - one strain	70	24	0.976	
cat	one ARG - one strain	all ARGs - all strains	70	24	0.976	
cat	one ARG - all strains	all ARGs - one strain	24	24	0.976	
cat	one ARG - all strains	all ARGs - all strains	24	24	0.976	
cat	all ARGs - one strain	all ARGs - all strains	24	24	0.976	
dfrA5	one ARG - one strain	one ARG - all strains	69	24	0.302	
dfrA5	one ARG - one strain	all ARGs - one strain	69	24	0.067	
dfrA5	one ARG - one strain	all ARGs - all strains	69	24	0.067	
dfrA5	one ARG - all strains	all ARGs - one strain	24	24	0.862	
dfrA5	one ARG - all strains	all ARGs - all strains	24	24	0.361	
dfrA5	all ARGs - one strain	all ARGs - all strains	24	24	0.361	

Supplementary Table 4. Wilcoxon test comparison between competition types for each strain (BH correction). The "Parent strain" column indicates the strain being tested, and the "Competition type x" column specifies the competition group compared. nX represents the number of replicates for each competition type. The raw p-values were adjusted using the Benjamini-Hochberg (BH) correction to control for the false discovery rate. Asterisks indicate the level of statistical significance for the strains between the competition types tested (*>0.05, **>0.01, ***>0.001, ****>0.0001).

Parent strain	Competition type 1	Competition type 2	n1	n2	Adjusted *p*-value (BH)	Significance
B156	one ARG - one strain	one ARG - all strains	68	24	0.849	ns
B156	one ARG - one strain	all ARGs - one strain	68	24	0.876	ns
B156	one ARG - one strain	all ARGs - all strains	68	24	0.0000774	****
B156	one ARG - all strains	all ARGs - one strain	24	24	0.865	ns
B156	one ARG - all strains	all ARGs - all strains	24	24	0.075	ns
B156	all ARGs - one strain	all ARGs - all strains	24	24	0.000213	***
B354	one ARG - one strain	one ARG - all strains	72	24	0.014	*
B354	one ARG - one strain	all ARGs - one strain	72	24	0.796	ns
B354	one ARG - one strain	all ARGs - all strains	72	24	0.005	**
B354	one ARG - all strains	all ARGs - one strain	24	24	0.017	*
B354	one ARG - all strains	all ARGs - all strains	24	24	0.397	ns
B354	all ARGs - one strain	all ARGs - all strains	24	24	0.009	**
H504	one ARG - one strain	one ARG - all strains	72	24	0.976	ns
H504	one ARG - one strain	all ARGs - one strain	72	24	0.976	ns
H504	one ARG - one strain	all ARGs - all strains	72	24	0.976	ns
H504	one ARG - all strains	all ARGs - one strain	24	24	0.976	ns
H504	one ARG - all strains	all ARGs - all strains	24	24	0.976	ns
H504	all ARGs - one strain	all ARGs - all strains	24	24	0.976	ns
H588	one ARG - one strain	one ARG - all strains	72	24	0.012	*
H588	one ARG - one strain	all ARGs - one strain	72	24	0.226	ns
H588	one ARG - one strain	all ARGs - all strains	72	24	0.615	ns
H588	one ARG - all strains	all ARGs - one strain	24	24	0.012	*
H588	one ARG - all strains	all ARGs - all strains	24	24	0.000852	***

H588	all ARGs - one strain	all ARGs - all strains	24	24	0.069	ns
M863	one ARG - one strain	one ARG - all strains	68	24	0.063	ns
M863	one ARG - one strain	all ARGs - one strain	68	24	0.418	ns
M863	one ARG - one strain	all ARGs - all strains	68	24	0.469	ns
M863	one ARG - all strains	all ARGs - one strain	24	24	0.022	*
M863	one ARG - all strains	all ARGs - all strains	24	24	0.277	ns
M863	all ARGs - one strain	all ARGs - all strains	24	24	0.277	ns
REL606	one ARG - one strain	one ARG - all strains	69	24	0.103	ns
REL606	one ARG - one strain	all ARGs - one strain	69	24	0.002	**
REL606	one ARG - one strain	all ARGs - all strains	69	24	0.000903	***
REL606	one ARG - all strains	all ARGs - one strain	24	24	0.097	ns
REL606	one ARG - all strains	all ARGs - all strains	24	24	0.199	ns
REL606	all ARGs - one strain	all ARGs - all strains	24	24	0.000903	***

REFERENCES

Alonso-del Valle, A., León-Sampedro, R., Rodríguez-Beltrán, J., DelaFuente, J., Hernández-García, M., Ruiz-Garbajosa, P., Cantón, R., Peña-Miller, R., & San Millán, A. (2021). Variability of plasmid fitness effects contributes to plasmid persistence in bacterial communities. *Nature Communications*, *12*(1), 2653. https://doi.org/10.1038/s41467-021-22849-y

Amazon Web Services. (2023). Benchmarking the Oxford Nanopore Technologies basecallers on AWS. https://aws.amazon.com/blogs/hpc/benchmarking-the-oxford-nanopore-technologies-basecallers-on-aws/

Andersson, D. I., & Hughes, D. (2010). Antibiotic resistance and its cost: is it possible to reverse resistance? *Nature Reviews Microbiology*, *8*(4), 260-271. https://doi.org/10.1038/nrmicro2319

Baichman-Kass, A., Song, T., & Friedman, J. (2023). Competitive interactions between culturable bacteria are highly non-additive. *eLife*, *12*, e83398. https://doi.org/10.7554/eLife.83398

Balbontín, R., Frazão, N., & Gordo, I. (2021). DNA Breaks-Mediated Fitness Cost Reveals RNase HI as a New Target for Selectively Eliminating Antibiotic-Resistant Bacteria. *Mol Biol Evol*, *38*(8), 3220-3234. https://doi.org/10.1093/molbev/msab093

Barrick, J., Deatherage, D., & Sowa, S. (2023). *FLP Recombination in E. coli.* https://barricklab.org/twiki/bin/view/Lab/ProcedureFLPFRTRecombination

Beaber, J. W., Hochhut, B., & Waldor, M. K. (2004). SOS response promotes horizontal dissemination of antibiotic resistance genes. *Nature*, *427*(6969), 72-74. https://doi.org/10.1038/nature02241

Beckman Coulter. (2023). *AMPure XP beads protocol: Cleanup and size selection*. Retrieved October 20 from https://www.beckman.com/reagents/genomic/cleanup-and-size-selection/pcr/ampure-xp-protocol

Bengtsson-Palme, J., Kristiansson, E., & Larsson, D. G. J. (2017). Environmental factors influencing the development and spread of antibiotic resistance. *FEMS Microbiology Reviews*, *42*(1). https://doi.org/10.1093/femsre/fux053

Bergstrom, C. T., Lipsitch, M., & Levin, B. R. (2000). Natural Selection, Infectious Transfer and the Existence Conditions for Bacterial Plasmids. *Genetics*, *155*(4), 1505-1519. https://doi.org/10.1093/genetics/155.4.1505

Blair, J. M. A., Webber, M. A., Baylay, A. J., Ogbolu, D. O., & Piddock, L. J. V. (2015). Molecular mechanisms of antibiotic resistance. *Nature Reviews Microbiology*, *13*(1), 42-51. https://doi.org/10.1038/nrmicro3380

Blundell, J. R., & Levy, S. F. (2014). Beyond genome sequencing: Lineage tracking with barcodes to study the dynamics of evolution, infection, and cancer. *Genomics*, *104*(6, Part A), 417-430. https://doi.org/https://doi.org/10.1016/j.ygeno.2014.09.005

Brüssow, H., Canchaya, C., & Hardt, W. D. (2004). Phages and the evolution of bacterial pathogens: from genomic rearrangements to lysogenic conversion. *Microbiol Mol Biol Rev*, *68*(3), 560-602, table of contents. https://doi.org/10.1128/mmbr.68.3.560-602.2004

Bush, K. (2012). Evolution of β-Lactamases: Past, Present, and Future. In T. J. Dougherty & M. J. Pucci (Eds.), *Antibiotic Discovery and Development* (pp. 427-453). Springer US. https://doi.org/10.1007/978-1-4614-1400-1_12

Bustin, S., & Nolan, T. (2017). Talking the talk, but not walking the walk: RT-qPCR as a paradigm for the lack of reproducibility in molecular research. *European Journal of Clinical Investigation*, *47*(10), 756-774. https://doi.org/https://doi.org/10.1111/eci.12801

Butaitė, E., Baumgartner, M., Wyder, S., & Kümmerli, R. (2017). Siderophore cheating and cheating resistance shape competition for iron in soil and freshwater Pseudomonas communities. *Nature Communications*, *8*(1), 414. https://doi.org/10.1038/s41467-017-00509-4

Cao, Z., Casabona, M. G., Kneuper, H., Chalmers, J. D., & Palmer, T. (2016). The type VII secretion system of Staphylococcus aureus secretes a nuclease toxin that targets competitor bacteria. *Nature Microbiology*, *2*(1), 16183. https://doi.org/10.1038/nmicrobiol.2016.183

Carattoli, A. (2013). Plasmids and the spread of resistance. *International Journal of Medical Microbiology*, *303*(6), 298-304. https://doi.org/https://doi.org/10.1016/j.ijmm.2013.02.001

Carrera Páez, L. C., Olivier, M., Gambino, A. S., Poklepovich, T., Aguilar, A. P., Quiroga, M. P., & Centrón, D. (2024). Sporadic clone Escherichia coli ST615 as a vector and reservoir for dissemination of crucial antimicrobial resistance genes. *Frontiers in Cellular and Infection Microbiology*, *14*. https://doi.org/10.3389/fcimb.2024.1368622

Carroll, A. C., & Wong, A. (2018). Plasmid persistence: costs, benefits, and the plasmid paradox. *Canadian Journal of Microbiology*, *64*(5), 293-304. https://doi.org/10.1139/cjm-2017-0609 %M 29562144

Chen, I., & Dubnau, D. (2004). DNA uptake during bacterial transformation. *Nature Reviews Microbiology*, *2*(3), 241-249. https://doi.org/10.1038/nrmicro844

Choi, K.-H., & Schweizer, H. P. (2006). mini-Tn7 insertion in bacteria with single attTn7 sites: example Pseudomonas aeruginosa. *Nature protocols*, *1*(1), 153-161.

Colizzi, E. S., & Hogeweg, P. (2016). High cost enhances cooperation through the interplay between evolution and self-organisation. *BMC Evolutionary Biology*, *16*(1), 31. https://doi.org/10.1186/s12862-016-0600-9

Concepción-Acevedo, J., Weiss, H. N., Chaudhry, W. N., & Levin, B. R. (2015). Malthusian Parameters as Estimators of the Fitness of Microbes: A Cautionary Tale about the Low Side of High Throughput. *PLoS ONE*, *10*(6), e0126915. https://doi.org/10.1371/journal.pone.0126915

De Gelder, L., Ponciano, J. M., Joyce, P., & Top, E. M. (2007). Stability of a promiscuous plasmid in different hosts: no guarantee for a long-term relationship. *Microbiology*, *153*(2), 452-463. https://doi.org/https://doi.org/10.1099/mic.0.2006/001784-0

de Souza, J., Vieira, A. Z., dos Santos, H. G., & Faoro, H. (2024). Potential involvement of beta-lactamase homologous proteins in resistance to beta-lactam antibiotics in gram-negative bacteria of the ESKAPEE group. *BMC Genomics*, *25*(1), 508. https://doi.org/10.1186/s12864-024-10410-2

Deng, C., Liu, X., Li, L., Shi, J., Guo, W., & Xue, J. (2020). Temporal dynamics of antibiotic resistant genes and their association with the bacterial community in a water-sediment mesocosm under selection by 14 antibiotics. *Environment International*, *137*, 105554. https://doi.org/https://doi.org/10.1016/j.envint.2020.105554

diCenzo, G. C., MacLean, A. M., Milunovic, B., Golding, G. B., & Finan, T. M. (2014). Examination of Prokaryotic Multipartite Genome Evolution through Experimental

Genome Reduction. *PLoS Genetics*, *10*(10), e1004742. https://doi.org/10.1371/journal.pgen.1004742

Duan, Y., Chen, Z., Tan, L., Wang, X., Xue, Y., Wang, S., Wang, Q., Das, R., Lin, H., Hou, J., Li, L., Mao, D., & Luo, Y. (2020). Gut resistomes, microbiota and antibiotic residues in Chinese patients undergoing antibiotic administration and healthy individuals. *Science of the Total Environment*, *705*, 135674. https://doi.org/10.1016/j.scitotenv.2019.135674

Dunn, S., Carrilero, L., Brockhurst, M., & McNally, A. (2021). Limited and Strain-Specific Transcriptional and Growth Responses to Acquisition of a Multidrug Resistance Plasmid in Genetically Diverse Escherichia coli Lineages. *mSystems*, *6*(2), 10.1128/msystems.00083-00021. https://doi.org/doi:10.1128/msystems.00083-21

Durão, P., Balbontín, R., & Gordo, I. (2018). Evolutionary Mechanisms Shaping the Maintenance of Antibiotic Resistance. *Trends in Microbiology*, *26*(8), 677-691. https://doi.org/https://doi.org/10.1016/j.tim.2018.01.005

Ellabaan, M. M. H., Munck, C., Porse, A., Imamovic, L., & Sommer, M. O. A. (2021). Forecasting the dissemination of antibiotic resistance genes across bacterial genomes. *Nature Communications*, *12*(1), 2435. https://doi.org/10.1038/s41467-021-22757-1

Fay, A., Philip, J., Saha, P., Hendrickson Ronald, C., Glickman Michael, S., & Burns-Huang, K. (2021). The DnaK Chaperone System Buffers the Fitness Cost of Antibiotic Resistance Mutations in Mycobacteria. *mBio*, *12*(2), 10.1128/mbio.00123-00121. https://doi.org/10.1128/mbio.00123-21

Galgano, M., Pellegrini, F., Catalano, E., Capozzi, L., Del Sambro, L., Sposato, A., Lucente, M. S., Vasinioti, V. I., Catella, C., Odigie, A. E., Tempesta, M., Pratelli, A., & Capozza, P. (2025). Acquired Bacterial Resistance to Antibiotics and Resistance Genes: From Past to Future. *Antibiotics*, *14*(3), 222.

García-Solache, M., & Rice, L. B. (2019). The Enterococcus: a Model of Adaptability to Its Environment. *Clinical Microbiology Reviews*, *32*(2), 10.1128/cmr.00058-00018. https://doi.org/doi:10.1128/cmr.00058-18

Geesink, P., Ter Horst, J., & Ettema, T. J. G. (2024). More than the sum of its parts: uncovering emerging effects of microbial interactions in complex communities. *FEMS Microbiol Ecol*, *100*(4). https://doi.org/10.1093/femsec/fiae029

Gerdes, K., Rasmussen, P. B., & Molin, S. (1986). Unique type of plasmid maintenance function: postsegregational killing of plasmid-free cells. *Proceedings of the National Academy of Sciences*, *83*(10), 3116-3120. https://doi.org/doi:10.1073/pnas.83.10.3116

Gifford, D. R., Berríos-Caro, E., Joerres, C., Suñé, M., Forsyth, J. H., Bhattacharyya, A., Galla, T., & Knight, C. G. (2023). Mutators can drive the evolution of multi-resistance to antibiotics. *PLoS Genetics*, *19*(6), e1010791. https://doi.org/10.1371/journal.pgen.1010791

Gomes, T. A. T., Ooka, T., Hernandes, R. T., Yamamoto, D., & Hayashi, T. (2020). Escherichia albertii Pathogenesis. *EcoSal Plus*, *9*(1). https://doi.org/10.1128/ecosalplus.ESP-0015-2019

Hall, J. P. J., Harrison, E., Lilley, A. K., Paterson, S., Spiers, A. J., & Brockhurst, M. A. (2015). Environmentally co-occurring mercury resistance plasmids are genetically and phenotypically diverse and confer variable context-dependent fitness effects.

Environmental Microbiology, *17*(12), 5008-5022. https://doi.org/https://doi.org/10.1111/1462-2920.12901

Hall, J. P. J., Harrison, E., Pärnänen, K., Virta, M., & Brockhurst, M. A. (2020). The Impact of Mercury Selection and Conjugative Genetic Elements on Community Structure and Resistance Gene Transfer. *Frontiers in Microbiology*, *11*. https://doi.org/10.3389/fmicb.2020.01846

Hall, J. P. J., Wright, R. C. T., Harrison, E., Muddiman, K. J., Wood, A. J., Paterson, S., & Brockhurst, M. A. (2021). Plasmid fitness costs are caused by specific genetic conflicts enabling resolution by compensatory mutation. *PLoS Biol*, *19*(10), e3001225. https://doi.org/10.1371/journal.pbio.3001225

Händel, N., Schuurmans, J. M., Feng, Y., Brul, S., & ter Kuile, B. H. (2014). Interaction between mutations and regulation of gene expression during development of de novo antibiotic resistance. *Antimicrob Agents Chemother*, *58*(8), 4371-4379. https://doi.org/10.1128/aac.02892-14

Harrison, E., Guymer, D., Spiers, Andrew J., Paterson, S., & Brockhurst, Michael A. (2015). Parallel Compensatory Evolution Stabilizes Plasmids across the Parasitism-Mutualism Continuum. *Current Biology*, *25*(15), 2034-2039. https://doi.org/https://doi.org/10.1016/j.cub.2015.06.024

Hegreness, M., Shoresh, N., Hartl, D., & Kishony, R. (2006). An Equivalence Principle for the Incorporation of Favorable Mutations in Asexual Populations. *Science*, *311*(5767), 1615-1617. https://doi.org/doi:10.1126/science.1122469

Hernandez-Beltran, J. C. R., Rodríguez-Beltrán, J., Aguilar-Luviano, O. B., Velez-Santiago, J., Mondragón-Palomino, O., MacLean, R. C., Fuentes-Hernández, A., San Millán, A., & Peña-Miller, R. (2024). Plasmid-mediated phenotypic noise leads to transient antibiotic resistance in bacteria. *Nature Communications*, *15*(1), 2610. https://doi.org/10.1038/s41467-024-45045-0

Hernando-Amado, S., Sanz-García, F., Blanco, P., & Martínez, José L. (2017). Fitness costs associated with the acquisition of antibiotic resistance. *Essays in Biochemistry*, *61*(1), 37-48. https://doi.org/10.1042/ebc20160057

Heuer, H., Binh, C. T., Jechalke, S., Kopmann, C., Zimmerling, U., Krögerrecklenfort, E., Ledger, T., González, B., Top, E., & Smalla, K. (2012). IncP-1ε Plasmids are Important Vectors of Antibiotic Resistance Genes in Agricultural Systems: Diversification Driven by Class 1 Integron Gene Cassettes. *Front Microbiol*, *3*, 2. https://doi.org/10.3389/fmicb.2012.00002

Hibbing, M. E., Fuqua, C., Parsek, M. R., & Peterson, S. B. (2010). Bacterial competition: surviving and thriving in the microbial jungle. *Nat Rev Microbiol*, *8*(1), 15-25. https://doi.org/10.1038/nrmicro2259

Hillmann, B., Al-Ghalith, G. A., Shields-Cutler, R. R., Zhu, Q., Gohl, D. M., Beckman, K. B., Knight, R., & Knights, D. (2018). Evaluating the Information Content of Shallow Shotgun Metagenomics. *mSystems*, *3*(6), 10.1128/msystems.00069-00018. https://doi.org/doi:10.1128/msystems.00069-18

Hirsch, P. R. (1979). Plasmid-determined Bacteriocin Production by Rhizobium leguminosarum. *Microbiology*, *113*(2), 219-228. https://doi.org/https://doi.org/10.1099/00221287-113-2-219

Hu, Y., Gao, G. F., & Zhu, B. (2017). The antibiotic resistome: gene flow in environments, animals and human beings. *Frontiers of Medicine*, *11*(2), 161-168. https://doi.org/10.1007/s11684-017-0531-x

Hughes, D., & Andersson, D. I. (2015). Evolutionary consequences of drug resistance: shared principles across diverse targets and organisms. *Nature Reviews Genetics*, *16*(8), 459-471. https://doi.org/10.1038/nrg3922

Humphrey, B., Thomson, N. R., Thomas, C. M., Brooks, K., Sanders, M., Delsol, A. A., Roe, J. M., Bennett, P. M., & Enne, V. I. (2012). Fitness of Escherichia coli strains carrying expressed and partially silent IncN and IncP1 plasmids. *BMC Microbiology*, *12*(1), 53. https://doi.org/10.1186/1471-2180-12-53

Jasinska, W., Manhart, M., Lerner, J., Gauthier, L., Serohijos, A. W. R., & Bershtein, S. (2020). Chromosomal barcoding of E. coli populations reveals lineage diversity dynamics at high resolution. *Nature Ecology & Evolution*, *4*(3), 437-452. https://doi.org/10.1038/s41559-020-1103-z

Kim, I. S. (2023). DNA Barcoding Technology for Lineage Recording and Tracing to Resolve Cell Fate Determination. *Cells*, *13*(1). https://doi.org/10.3390/cells13010027

Kottara, A., Hall, J. P. J., & Brockhurst, M. A. (2021). The proficiency of the original host species determines community-level plasmid dynamics. *FEMS Microbiology Ecology*, *97*(4). https://doi.org/10.1093/femsec/fiab026

Kvitek, D. J., & Sherlock, G. (2013). Whole Genome, Whole Population Sequencing Reveals That Loss of Signaling Networks Is the Major Adaptive Strategy in a Constant Environment. *PLoS Genetics*, *9*(11), e1003972. https://doi.org/10.1371/journal.pgen.1003972

Lai, H.-Y., & Cooper, T. F. (2024). Costs of antibiotic resistance genes depend on host strain and environment and can influence community composition. *Proceedings of the Royal Society B: Biological Sciences*, *291*(2025), 20240735. https://doi.org/doi:10.1098/rspb.2024.0735

Leclercq, R. (2002). Mechanisms of Resistance to Macrolides and Lincosamides: Nature of the Resistance Elements and Their Clinical Implications. *Clinical Infectious Diseases*, *34*(4), 482-492. https://doi.org/10.1086/324626

Lenski, R. E., Rose, M. R., Simpson, S. C., & Tadler, S. C. (1991). Long-Term Experimental Evolution in Escherichia coli. I. Adaptation and Divergence During 2,000 Generations. *The American Naturalist*, *138*(6), 1315-1341.

Levy, S. F., Blundell, J. R., Venkataram, S., Petrov, D. A., Fisher, D. S., & Sherlock, G. (2015). Quantitative evolutionary dynamics using high-resolution lineage tracking. *Nature*, *519*(7542), 181-186. https://doi.org/10.1038/nature14279

Li, X. Z., & Nikaido, H. (2009). Efflux-mediated drug resistance in bacteria: an update. *Drugs*, *69*(12), 1555-1623. https://doi.org/10.2165/11317030-000000000-00000

Liang, L., Zhong, L.-L., Wang, L., Zhou, D., Li, Y., Li, J., Chen, Y., Liang, W., Wei, W., Zhang, C., Zhao, H., Lyu, L., Stoesser, N., Doi, Y., Bai, F., Feng, S., & Tian, G.-B. (2023). A new variant of the colistin resistance gene MCR-1 with co-resistance to β-lactam antibiotics reveals a potential novel antimicrobial peptide. *PLoS Biology*, *21*(12), e3002433. https://doi.org/10.1371/journal.pbio.3002433

Loo, M. P. J. (2014). The stringdist Package for Approximate String Matching. *R Journal*, *6*, 111-122. https://doi.org/10.32614/RJ-2014-011

Luo, C., Walk, S., Gordon, D., Feldgarden, M., Tiedje, J., & Konstantinidis, K. (2011). Genome sequencing of environmental Escherichia coli expands understanding of the ecology and speciation of the model bacterial species. *Proceedings of the National Academy of Sciences of the United States of America*, *108*, 7200-7205. https://doi.org/10.1073/pnas.1015622108

Machuca, J., Briales, A., Labrador, G., Díaz-de-Alba, P., López-Rojas, R., Docobo-Pérez, F., Martínez-Martínez, L., Rodríguez-Baño, J., Pachón, M. E., Pascual, Á., & Rodríguez-Martínez, J.-M. (2014). Interplay between plasmid-mediated and chromosomal-mediated fluoroquinolone resistance and bacterial fitness in Escherichia coli. *Journal of Antimicrobial Chemotherapy*, *69*(12), 3203-3215. https://doi.org/10.1093/jac/dku308

Martínez, J. L., Coque, T. M., & Baquero, F. (2015). What is a resistance gene? Ranking risk in resistomes. *Nature Reviews Microbiology*, *13*(2), 116-123. https://doi.org/10.1038/nrmicro3399

Mee, M. T., Collins, J. J., Church, G. M., & Wang, H. H. (2014). Syntrophic exchange in synthetic microbial communities. *Proceedings of the National Academy of Sciences*, *111*(20), E2149-E2156. https://doi.org/doi:10.1073/pnas.1405641111

Melnyk, A. H., Wong, A., & Kassen, R. (2015). The fitness costs of antibiotic resistance mutations. *Evol Appl*, *8*(3), 273-283. https://doi.org/10.1111/eva.12196

Millan, A. S., & MacLean, R. C. (2017). Fitness Costs of Plasmids: a Limit to Plasmid Transmission. *Microbiology Spectrum*, *5*(5), 5.5.02. https://doi.org/doi:10.1128/microbiolspec.mtbp-0016-2017

Miranda, S. W., Asfahl, K. L., Dandekar, A. A., & Greenberg, E. P. (2022). Pseudomonas aeruginosa Quorum Sensing. *Adv Exp Med Biol*, *1386*, 95-115. https://doi.org/10.1007/978-3-031-08491-1_4

Morris, B. E. L., Henneberger, R., Huber, H., & Moissl-Eichinger, C. (2013). Microbial syntrophy: interaction for the common good. *FEMS Microbiology Reviews*, *37*(3), 384-406. https://doi.org/10.1111/1574-6976.12019

Nair, R. R., & Andersson, D. I. (2023). Interspecies interaction reduces selection for antibiotic resistance in Escherichia coli. *Communications Biology*, *6*(1), 331. https://doi.org/10.1038/s42003-023-04716-2

Nguyen Ba, A. N., Cvijović, I., Rojas Echenique, J. I., Lawrence, K. R., Rego-Costa, A., Liu, X., Levy, S. F., & Desai, M. M. (2019). High-resolution lineage tracking reveals travelling wave of adaptation in laboratory yeast. *Nature*, *575*(7783), 494-499. https://doi.org/10.1038/s41586-019-1749-3

Ni, Y., Liu, X., Simeneh, Z. M., Yang, M., & Li, R. (2023). Benchmarking of Nanopore R10.4 and R9.4.1 flow cells in single-cell whole-genome amplification and whole-genome shotgun sequencing. *Computational and Structural Biotechnology Journal*, *21*, 2352-2364. https://doi.org/https://doi.org/10.1016/j.csbj.2023.03.038

Nordstrom, K., & Austin, S. J. (1989). MECHANISMS THAT CONTRIBUTE TO THE STABLE SEGREGATION OF PLASMIDS. *Annual Review of Genetics*, *23*, 37-69. https://doi.org/10.1146/annurev.ge.23.120189.000345

Oaks, J. L., Besser, T. E., Walk, S. T., Gordon, D. M., Beckmen, K. B., Burek, K. A., Haldorson, G. J., Bradway, D. S., Ouellette, L., Rurangirwa, F. R., Davis, M. A., Dobbin, G., & Whittam, T. S. (2010). Escherichia albertii in wild and domestic birds. *Emerg Infect Dis*, *16*(4), 638-646. https://doi.org/10.3201/eid1604.090695

Oresnik, I. J., Liu, S.-L., Yost, C. K., & Hynes, M. F. (2000). Megaplasmid pRme2011a of Sinorhizobium meliloti Is Not Required for Viability. *Journal of Bacteriology*, *182*(12), 3582-3586. https://doi.org/doi:10.1128/jb.182.12.3582-3586.2000

Oxford Nanopore Technologies. (2023). *London Calling 2023: Technology update* https://nanoporetech.com/resource-centre/london-calling-2023-technology-update

Oxford Nanopore Technologies. (2024). *Dorado*. In https://github.com/nanoporetech/dorado

Pacheco, J. O., Alvarez-Ortega, C., Rico, M. A., & Martínez, J. L. (2017). Metabolic Compensation of Fitness Costs Is a General Outcome for Antibiotic-Resistant Pseudomonas aeruginosa Mutants Overexpressing Efflux Pumps. *mBio*, *8*(4), 10.1128/mbio.00500-00517. https://doi.org/doi:10.1128/mbio.00500-17

Parker, E. M., Ballash, G. A., Mollenkopf, D. F., & Wittum, T. E. (2024). A complex cyclical One Health pathway drives the emergence and dissemination of antimicrobial resistance. *American Journal of Veterinary Research*, *85*(4), ajvr.24.01.0014. https://doi.org/10.2460/ajvr.24.01.0014

Partridge, S. R., Kwong, S. M., Firth, N., & Jensen, S. O. (2018). Mobile Genetic Elements Associated with Antimicrobial Resistance. *Clin Microbiol Rev*, *31*(4). https://doi.org/10.1128/cmr.00088-17

Platt, T. G., Bever, J. D., & Fuqua, C. (2012). A cooperative virulence plasmid imposes a high fitness cost under conditions that induce pathogenesis. *Proceedings of the Royal Society B: Biological Sciences*, *279*(1734), 1691-1699. https://doi.org/doi:10.1098/rspb.2011.2002

Poole, K. (2007). Efflux pumps as antimicrobial resistance mechanisms. *Annals of Medicine*, *39*(3), 162-176. https://doi.org/10.1080/07853890701195262

Qi, Q., Kamruzzaman, M., & Iredell, J. R. (2021). The higBA-Type Toxin-Antitoxin System in IncC Plasmids Is a Mobilizable Ciprofloxacin-Inducible System. *mSphere*, *6*(3), 10.1128/msphere.00424-00421. https://doi.org/doi:10.1128/msphere.00424-21

Quince, C., Walker, A. W., Simpson, J. T., Loman, N. J., & Segata, N. (2017). Shotgun metagenomics, from sampling to analysis. *Nature Biotechnology*, *35*(9), 833-844. https://doi.org/10.1038/nbt.3935

Rajer, F., Sandegren, L., & Cooper, V. S. (2022). The Role of Antibiotic Resistance Genes in the Fitness Cost of Multiresistance Plasmids. *mBio*, *13*(1), e03552-03521. https://doi.org/doi:10.1128/mbio.03552-21

Ramirez, M. S., & Tolmasky, M. E. (2010). Aminoglycoside modifying enzymes. *Drug Resist Updat*, *13*(6), 151-171. https://doi.org/10.1016/j.drup.2010.08.003

Ramiro-Martínez, P., de Quinto, I., Lanza, V. F., Gama, J. A., & Rodríguez-Beltrán, J. (2025). Universal rules govern plasmid copy number. *Nature Communications*, *16*(1), 6022. https://doi.org/10.1038/s41467-025-61202-5

Rouch, D. A., Lee, B. T., & Morby, A. P. (1995). Understanding cellular responses to toxic agents: a model for mechanism-choice in bacterial metal resistance. *J Ind Microbiol*, *14*(2), 132-141. https://doi.org/10.1007/bf01569895

Samarakoon, H., Ferguson, J. M., Gamaarachchi, H., & Deveson, I. W. (2023). Accelerated nanopore basecalling with SLOW5 data format. *Bioinformatics*, *39*(6). https://doi.org/10.1093/bioinformatics/btad352

Sánchez, M. B., & Martínez, J. L. (2012). Differential Epigenetic Compatibility of qnr Antibiotic Resistance Determinants with the Chromosome of Escherichia coli. *PLoS ONE*, *7*(5), e35149. https://doi.org/10.1371/journal.pone.0035149

Sandoz, K. M., Mitzimberg, S. M., & Schuster, M. (2007). Social cheating in Pseudomonas aeruginosa quorum sensing. *Proc Natl Acad Sci U S A*, *104*(40), 15876-15881. https://doi.org/10.1073/pnas.0705653104

Scholz, S. A., Diao, R., Wolfe, M. B., Fivenson, E. M., Lin, X. N., & Freddolino, P. L. (2019). High-Resolution Mapping of the Escherichia coli Chromosome Reveals Positions of High and Low Transcription. *Cell Syst*, *8*(3), 212-225.e219. https://doi.org/10.1016/j.cels.2019.02.004

Sereika, M., Kirkegaard, R. H., Karst, S. M., Michaelsen, T. Y., Sørensen, E. A., Wollenberg, R. D., & Albertsen, M. (2022). Oxford Nanopore R10.4 long-read sequencing enables the generation of near-finished bacterial genomes from pure cultures and metagenomes without short-read or reference polishing. *Nature Methods*, *19*(7), 823-826. https://doi.org/10.1038/s41592-022-01539-7

Silver, S. (1992). Plasmid-determined metal resistance mechanisms: Range and overview. *Plasmid*, *27*(1), 1-3. https://doi.org/https://doi.org/10.1016/0147-619X(92)90001-Q

Smillie, C., Garcillán-Barcia, M. P., Francia, M. V., Rocha, E. P., & de la Cruz, F. (2010). Mobility of plasmids. *Microbiol Mol Biol Rev*, *74*(3), 434-452. https://doi.org/10.1128/mmbr.00020-10

Song, F., Kuehl, J. V., Chandran, A., & Arkin, A. P. (2021). A Simple, Cost-Effective, and Automation-Friendly Direct PCR Approach for Bacterial Community Analysis. *mSystems*, *6*(5), 10.1128/msystems.00224-00221. https://doi.org/doi:10.1128/msystems.00224-21

Stirling, F., Bitzan, L., O'Keefe, S., Redfield, E., Oliver, J. W. K., Way, J., & Silver, P. A. (2017). Rational Design of Evolutionarily Stable Microbial Kill Switches. *Mol Cell*, *68*(4), 686-697.e683. https://doi.org/10.1016/j.molcel.2017.10.033

Sun, S., Selmer, M., & Andersson, D. I. (2014). Resistance to β-Lactam Antibiotics Conferred by Point Mutations in Penicillin-Binding Proteins PBP3, PBP4 and PBP6 in Salmonella enterica. *PLoS ONE*, *9*(5), e97202. https://doi.org/10.1371/journal.pone.0097202

Sünderhauf, D., Klümper, U., Gaze, W. H., Westra, E. R., & van Houte, S. (2023). Interspecific competition can drive plasmid loss from a focal species in a microbial community. *Isme j*, *17*(10), 1765-1773. https://doi.org/10.1038/s41396-023-01487-w

Theodosiou, L., Farr, A. D., & Rainey, P. B. (2023). Barcoding Populations of Pseudomonas fluorescens SBW25. *J Mol Evol*, *91*(3), 254-262. https://doi.org/10.1007/s00239-023-10103-6

Thielecke, L., Cornils, K., & Glauche, I. (2019). genBaRcode: a comprehensive R-package for genetic barcode analysis. *Bioinformatics*, *36*(7), 2189-2194. https://doi.org/10.1093/bioinformatics/btz872

Tu, Q., Yin, J., Fu, J., Herrmann, J., Li, Y., Yin, Y., Stewart, A. F., Müller, R., & Zhang, Y. (2016). Room temperature electrocompetent bacterial cells improve DNA transformation and recombineering efficiency. *Scientific Reports*, *6*(1), 24648. https://doi.org/10.1038/srep24648

Van Melderen, L., & Saavedra De Bast, M. (2009). Bacterial Toxin–Antitoxin Systems: More Than Selfish Entities? *PLoS Genetics*, *5*(3), e1000437. https://doi.org/10.1371/journal.pgen.1000437

Vogwill, T., Kojadinovic, M., & MacLean, R. C. (2016). Epistasis between antibiotic resistance mutations and genetic background shape the fitness effect of resistance across species of Pseudomonas. *Proceedings of the Royal Society B: Biological Sciences*, *283*(1830), 20160151. https://doi.org/doi:10.1098/rspb.2016.0151

Vogwill, T., & MacLean, R. C. (2015). The genetic basis of the fitness costs of antimicrobial resistance: a meta-analysis approach. *Evolutionary Applications*, *8*(3), 284-295. https://doi.org/https://doi.org/10.1111/eva.12202

von Wintersdorff, C. J. H., Penders, J., van Niekerk, J. M., Mills, N. D., Majumder, S., van Alphen, L. B., Savelkoul, P. H. M., & Wolffs, P. F. G. (2016). Dissemination of Antimicrobial Resistance in Microbial Ecosystems through Horizontal Gene Transfer. *Frontiers in Microbiology*, *7*. https://doi.org/10.3389/fmicb.2016.00173

Walk, S. T., Alm, E. W., Gordon, D. M., Ram, J. L., Toranzos, G. A., Tiedje, J. M., & Whittam, T. S. (2009). Cryptic lineages of the genus Escherichia. *Appl Environ Microbiol*, *75*(20), 6534-6544. https://doi.org/10.1128/aem.01262-09

Wang, Y., Diaz Arenas, C., Stoebel, D. M., Flynn, K., Knapp, E., Dillon, M. M., Wünsche, A., Hatcher, P. J., Moore, F. B.-G., Cooper, V. S., & Cooper, T. F. (2016). Benefit of transferred mutations is better predicted by the fitness of recipients than by their ecological or genetic relatedness. *Proceedings of the National Academy of Sciences*, *113*(18), 5047-5052. https://doi.org/doi:10.1073/pnas.1524988113

Wang, Y., Wang, C., & Song, L. (2019). Distribution of antibiotic resistance genes and bacteria from six atmospheric environments: Exposure risk to human. *Science of the Total Environment*, *694*, 133750. https://doi.org/10.1016/j.scitotenv.2019.133750

Wardell, G. E., Hynes, M. F., Young, P. J., & Harrison, E. (2022). Why are rhizobial symbiosis genes mobile? *Philosophical Transactions of the Royal Society B: Biological Sciences*, *377*(1842), 20200471. https://doi.org/doi:10.1098/rstb.2020.0471

Xiong, W., Sun, Y., Ding, X., Wang, M., & Zeng, Z. (2015). Selective pressure of antibiotics on ARGs and bacterial communities in manure-polluted freshwater-sediment microcosms. *Frontiers in Microbiology*, *6*. https://doi.org/10.3389/fmicb.2015.00194

Zaslaver, A., Bren, A., Ronen, M., Itzkovitz, S., Kikoin, I., Shavit, S., Liebermeister, W., Surette, M. G., & Alon, U. (2006). A comprehensive library of fluorescent transcriptional reporters for Escherichia coli. *Nature Methods*, *3*(8), 623-628. https://doi.org/10.1038/nmeth895

Zhuang, M., Achmon, Y., Cao, Y., Liang, X., Chen, L., Wang, H., Siame, B. A., & Leung, K. Y. (2021). Distribution of antibiotic resistance genes in the environment. *Environmental Pollution*, *285*, 117402. https://doi.org/10.1016/j.envpol.2021.117402 (Environmental Pollution)